Research Square

Preprints are preliminary reports that have not undergone peer review.
They should not be considered conclusive, used to inform clinical practice,
or referenced by the media as validated information.

Why Wetland Restoration Cannot Fully Recover Lost Flood Protection: Evidence from SWAT+ Based Watershed Modelling

L.O.H. Perera
University of Moratuwa
E.J. Warusavitharana
emeshi@uom.lk

University of Moratuwa https://orcid.org/0000-0002-0352-2926

Research Article

Keywords: Wetland Degradation and Restoration, SWAT+ Hydrological Modelling, Flood Attenuation, Non-linearity, Complex Adaptive System, Hysteresis

Posted Date: May 18th, 2026

DOI: https://doi.org/10.21203/rs.3.rs-9340656/v1

License: This work is licensed under a Creative Commons Attribution 4.0 International License.
Read Full License

Why Wetland Restoration Cannot Fully Recover Lost Flood Protection: Evidence from SWAT+ Based Watershed Modelling

L.O.H. Perera[1], and E.J. Warusavitharana[1*]

[1] Department of Town & Country Planning, Faculty of Architecture, University of Moratuwa, Bandaranayake Mawatha, Moratuwa 10400, Sri Lanka

***Corresponding Author**: emeshi@uom.lk

Abstract

Wetlands provide critical ecosystem services by regulating hydrological processes and moderating flood risks. However, gradual wetland degradation often occurs through small-scale land conversions that remain below regulatory thresholds, leading to cumulative impacts on watershed stability. Despite growing recognition of these pressures, most hydrological assessments evaluate wetlands using simplified "with–without" comparisons, which fail to capture nonlinear responses associated with incremental loss and restoration. This study develops a watershed-scale modelling framework to investigate how progressive wetland degradation and restoration influence flood attenuation services within a complex hydrological system. A calibrated SWAT+ modelling framework was used to simulate a series of wetland loss and restoration scenarios ranging from 5% to 90% of existing wetland extent.

The results show a strong nonlinear relationship between wetland loss and flood response. Peak discharge increases progressively with wetland loss, with a clear acceleration beyond approximately 25–30% loss, suggesting the existence of a critical threshold beyond which watershed stability deteriorates rapidly. In contrast, restoration scenarios reveal significant hysteresis behaviour. Equivalent restoration efforts recover only a limited portion of the lost flood attenuation capacity, demonstrating that hydrological systems exhibit path dependency and memory effects. Quantitative assessment shows that less than half of the cumulative hydrological impacts generated during degradation can be reversed through comparable restoration measures.

Keywords: Wetland Degradation and Restoration, SWAT+ Hydrological Modelling, Flood Attenuation, Non-linearity, Complex Adaptive System, Hysteresis

1. INTRODUCTION

Despite extensive scientific evidence demonstrating the hydrological importance of wetlands, and the existence of legal and regulatory frameworks intended to protect them, wetlands continue to decline globally at alarming rates. The Ramsar Global Wetland Outlook estimates that approximately 411 million hectares (22% of global wetland area) have been lost since 1970, with roughly one-quarter of remaining wetlands now degraded. Studies across Asia have documented peak discharge increases of up to 50% following conversion of paddy wetlands to urban land cover (Hao et al., 2015). Historical reconstructions indicate cumulative losses of 30–60% of original wetland area across many regions, driven primarily by urban expansion, agricultural conversion, and infrastructure development, with Asia identified as a prominent hotspot (Yi et al., 2024).

Wetlands represent diverse range of landscape forms, including marshes, swamps, peatlands, mangroves, floodplains, and seasonally inundated paddy fields (Mitsch & Gosselink, 2015). The Ramsar Convention's inclusive definition recognizes both natural and anthropogenic water-retaining environments (Davis et al., 1997), which is particularly relevant in South Asian contexts where paddy fields function as ecologically significant artificial wetlands. In Sri Lanka, approximately 15% of land area comprises wetlands, with over half being man-made systems including reservoirs and paddy fields (IUCN, 2004). Significant declines in functioning of wetland environments can be caused by cumulative effect of individually insignificant actions. It directs to the systemic failure of planning and regulatory frameworks to effectively address this piecemeal degradation. Degradation of the hydrologic integrity of a watershed is decided by the gradual, fragmented destruction of small, retention landscapes, including both marshes and paddy fields (McMillian, 2022). This piecemeal degradation exposes a fundamental flaw in the existing regulatory framework. In Sri Lanka, the primary process for environmental governance is the project-specific Environmental Impact Assessment (EIA). The National Environment Act (Gazette No. 772/22 dated 24.06.1993) states that an EIA is required only if the area required for the project exceeds 4 hectares of natural wetland. Although there is no specific EIA procedure for projects requiring the reclamation of paddy fields, several prohibitions have been set out for the reclamation of paddy fields under the Agrarian Development Act No. 46 of 2000. However, paddy fields are not considered or treated as wetland environments under the existing regulations in Sri Lanka. In Sri Lanka and many Asian regions, paddy landscapes function as managed storage systems that contribute to flood moderation and groundwater recharge (Kudo et al., 2015). Although detailed models exist for paddy water management (Xia et al., 2022), watershed scale assessments often treat all wetlands as a single category (Mukherjee et al., 2021). The separate and combined contributions of natural wetlands and paddy systems to nonlinear flood regulation therefore remain insufficiently examined.

A substantial body of literature exists examining the role of wetlands in watershed hydrological processes. Much of this work has focused on sediment and nutrient dynamics within wetland systems (Qian et al., 2023; Page et al., 2023; Sohoulande, et al., 2022; Mereta et al., 2020; Jansson et al., 1998), as well as their capacity for water retention. Existing approaches to assessing wetland retention capacity include simplified mass-balance water budget models (Zhang & Mitsch, 2005), curve number (CN)-based methods (Chen et al., 2014; Dona et al., 2025), and algorithms derived from soil properties (Krnáčová et al., 2025). In addition, a range of hydrological modelling tools such as LISFLOOD-FP (2D), MIKE FLOOD, HEC-HMS, SWAT and SWMM have been widely applied to simulate wetland hydrological behaviour and flood dynamics (Padmanabhan & Bengtson, 2001; Wen et al., 2013; e Sousa & Miranda, 2018; Makungu & Hughes, 2021; Kumar et al., 2021; Bouzidi & Pérez-Blanco 2025). These

modelling approaches typically rely on simplified scenarios, such as “with” and “without” wetland conditions (Golden et al., 2014; Al-Attabi et al., 2023), rather than explicitly evaluating the gradual and cumulative effects of wetland degradation over time.

Further, numerous studies have shown that hydrological systems respond nonlinearly to land-use change and climate variability, with threshold-like behaviour and asymmetric changes in runoff and storage observed in deforestation, urbanization, and other land-cover transitions (Zehe & Sivapalan, 2009; ; Gentine et al., 2012; Schottler et al., 2014; Evenson et al. 2018; Vreugdenhil et al., 2022; Lopes et al., 2022). However, such nonlinear dynamics have received limited attention when examined specifically in relation to wetland loss. As a result, potential threshold behaviour linked specifically to progressive wetland loss remains insufficiently understood.

The ecosystem restoration literature indicates that the structural and functional recovery of wetlands is often slow and incomplete, frequently lagging behind reference conditions for decades (Jones et al., 2018; Cadier et al., 2020). However, while the ecological recovery of wetlands has been extensively quantified, hydrological functions, particularly flood attenuation is often assumed rather than explicitly measured in restoration assessments (Kadykalo & Findlay, 2016; Meli et al., 2014). In this context, the concept of hysteresis has been well established both theoretically and empirically, particularly in lakes and other dynamic ecosystems (Scheffer et al., 2001; Suding & Hobbs, 2009). Hysteresis describes a condition in which, even after restoration efforts are implemented, degraded ecosystems do not return to their original state, reflecting path dependency and system memory. Many existing ecosystem service models and spatially distributed hydrological models do not incorporate hysteresis or threshold dynamics, instead relying on assumptions of linear and reversible relationships between wetland extent and flood regulation capacity (Craft et al., 2003; Maes et al., 2024). As a result, the potential irreversibility of flood attenuation services under progressive wetland loss remains largely unexplored.

Under this circumstance, we hypothesized that (i) wetland loss exhibits a nonlinear relationship with peak discharge, with threshold behavior whereby small reductions beyond a critical limit lead to disproportionately large increases in flood risk; and (ii) watershed recovery exhibits hysteresis, such that restoration of equivalent wetland areas yields a smaller reduction in peak discharge than the increase caused by their loss, indicating path-dependent and non-reversible hydrological responses.

Accordingly, this study is structured around four primary objectives:

1. To develop and apply a calibrated hydrological modeling framework that identify natural marshes and paddy fields as distinct yet functionally interconnected hydrological units.
2. To quantify the retention capacities of existing wetland environments in each subbasin under extreme rainfall conditions.
3. To execute a series of simulation scenarios representing incremental wetland environment loss (5% to 90%) to analyze the non-linear hydrological response.
4. To execute a series of simulation scenarios representing incremental wetland environment restoration (5% to 90%) to investigate the hysteresis and system memory behavior of the watershed.

2. MATERIALS AND METHODS

The selected study area for this research is the Kelani River Basin, Sri Lanka, which comprises 20 sub-basins (Figure 1). This basin provides an ideal setting for examining flood attenuation services and hydrological resilience, as it encompasses major economic epicenters of the country, including Colombo and Gampaha. It is

home to a great mosaic of wetland systems, including major natural marshes - Thalangama Tank, Colombo Flood Retention Area, Kolonnawa Marsh, Mahara-Enderamulla Wetland, Biyagama, Kiribathgoda, Peliyagoda Wetland complex, Kimbulawala, and Madiwela Wetlands and an expanded paddy field system, which makes it ideal for the study. Quantitatively, 55.7% of the entire basin area has a slope of 0-5%, with this low-slope terrain being concentrated in the western sub-basins, making the area highly vulnerable to flooding (Mallawatantri, 2016). As urbanization expanded, from 1989 to 2016, natural marshes declined by 52% in the Kelani basin. Currently, wetlands occupy less than 1% of the total basin area, and the annual rate of reclamation increases 2.95% per year in the protected wetland areas (Surasinghe, et.al., 2019).

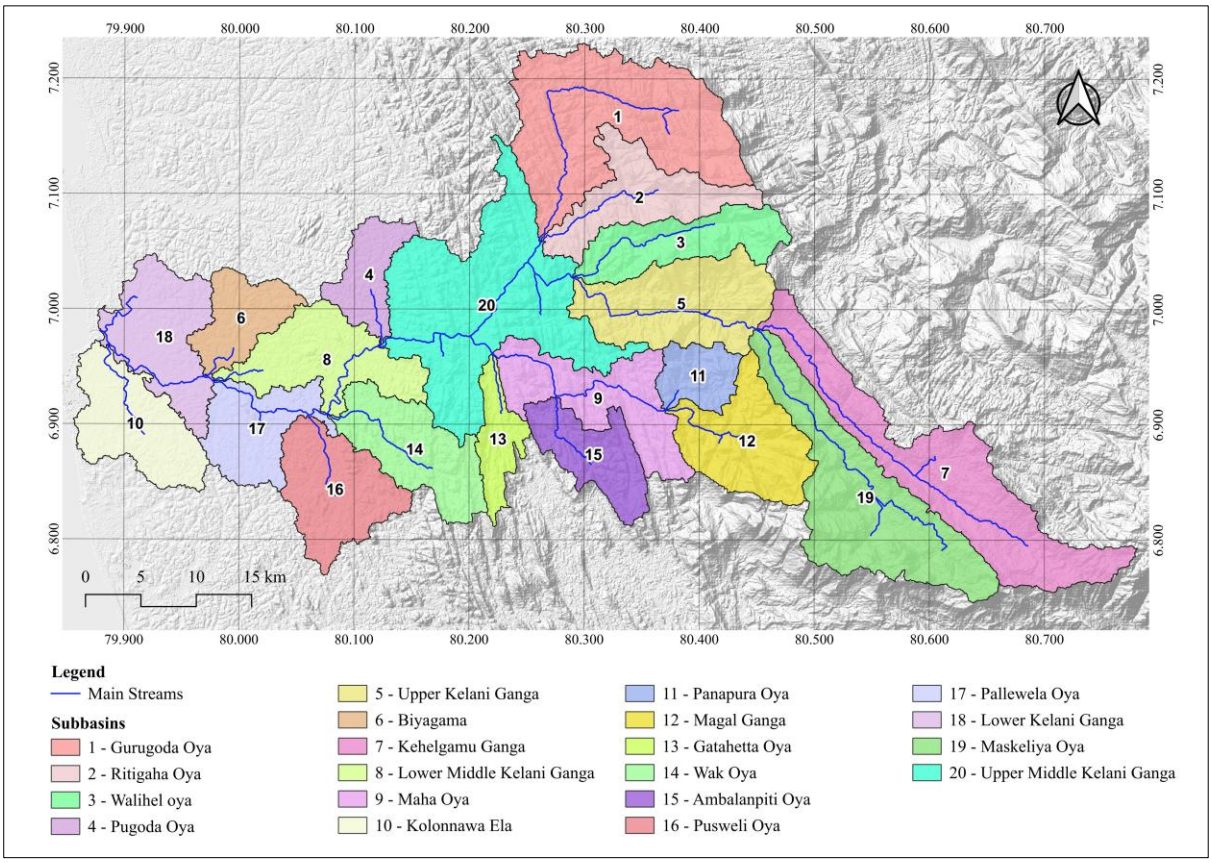


Figure 1: Kelani River Basin

For this study, the Soil and Water Assessment Tool Plus (SWAT+) modelling software has been used to simulate the hydrological processes in the watershed. Unlike the older SWAT version, which routed all water from the subbasin to channel outlets, SWAT+ allows runoff to flow from upland areas into floodplain areas before reaching the channel network. This feature allows the model to physically simulate the interception and retention of upland runoff by the wetland system. The modelling workflow integrated three software platforms: QSWAT+ for watershed delineation and HRU (Hydrological Response Units) creation within QGIS interface, SWAT+ Editor for model parameterization, simulation, and calibration, and SWAT+ Toolbox for sensitivity analysis. Table 1 shows the spatial and temporal datasets used in SWAT+ for hydrological model development.

Table 1: Spatial and temporal datasets used in SWAT+ model development

Input Data	Source	Remarks
Topography	Shuttle Radar Topography Mission (SRTM) Digital Elevation Model (DEM), 30 m spatial resolution	Used for watershed delineation, slope estimation, and stream network extraction
Land Use / Land Cover (LULC) (2024)	Generated using Random Forest classification in Google Earth Engine; validated against Google Earth Pro imagery, Google Dynamic World, and ESRI Sentinel-2 global land cover products	11 classes; overall accuracy = 86.93%; Kappa = 0.856; key classes: built-up (25.15%), rubber (33.14%), paddy (7.52%), marshlands (1.89%)
Soil Data	FAO World Soil Database; cross-referenced with Geological Survey and Mines Bureau (GSMB), Sri Lanka	Predominantly Hydrologic Soil Group C; slow infiltration and moderate runoff potential
Precipitation (2005–2024)	Irrigation Department of Sri Lanka (Hanwella, Glencourse, Kitulgala, Holombuwa, Deraniyagala stations)	Daily rainfall data used for model simulation
Other Climate Variables	Climate Forecast System Reanalysis (CFSR) global dataset	Temperature, relative humidity, solar radiation, and wind speed inputs
Weather Gap Filling	SWAT+ Weather Generator (WGN) module	Used to address data gaps beyond 2014
Streamflow (2005–2024)	Hanwella gauging station, Irrigation Department of Sri Lanka	Daily discharge data used for calibration and validation

This study conceptualizes the watershed as a Complex Adaptive System (CAS) (Figure 2), drawing on systems ecology and resilience theory developed by Levin (1998) and Holling (2001), to support the theoretical basis for analysing hydrological behaviour under changing wetland conditions. A CAS is defined as a system of interacting components whose overall behaviour emerges from dynamic interactions among physical, biological, and human subsystems. Within this framework, flood attenuation is treated as a system level response arising from interactions among multiple landscape elements and processes. A key characteristic of CAS framework is nonlinearity. In hydrological systems, this implies that progressive changes in wetland extent may produce disproportionate variations in flood response once critical limits related to storage capacity, soil saturation, or system connectivity are approached or exceeded (Phillips, 2003; Zehe & Sivapalan, 2009). To examine this behaviour in relation to Objective 3, a series of scenario-based simulations representing incremental wetland loss were developed, allowing the response of peak discharge and related hydrological indicators to be evaluated across a continuous gradient of wetland change.

The framework also incorporates the concept of hysteresis to analyse recovery dynamics associated with Objective 4. Hysteresis refers to the condition in which system recovery does not follow the same trajectory as degradation, resulting in delayed or incomplete restoration of system function even when the original drivers are reversed (Scheffer et al., 2001; Suding et al., 2003). In this study, restoration scenarios were designed to represent progressive reintroduction of wetland area following degradation, enabling comparison between degradation and recovery pathways. This approach allows the identification of path dependency in hydrological response, where the current state of the watershed is influenced by its historical trajectory.

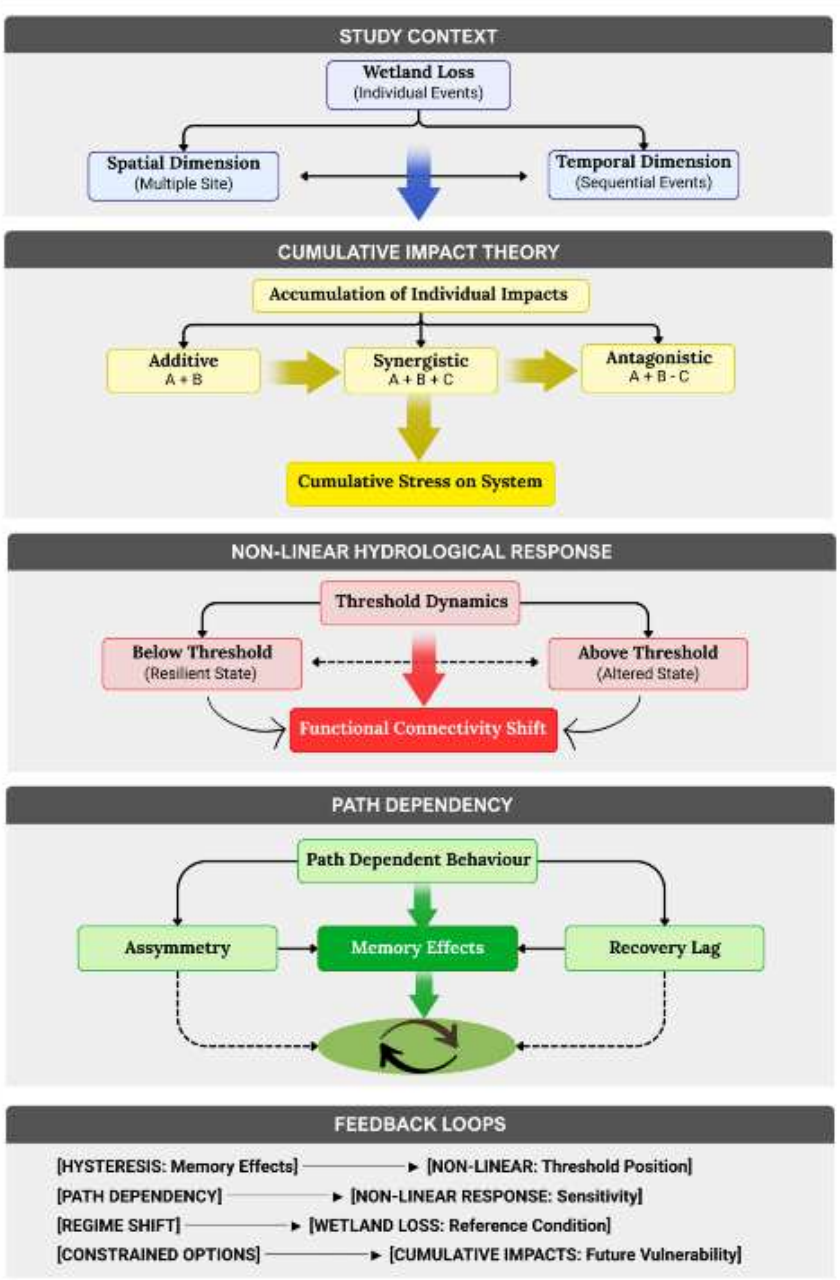


Figure 2: Conceptual Framework

As illustrated in Figure 3, Part 1 of the methodology details the hydrological model development process, including simulation, wetland representation, and model calibration and validation (Objective 1), while Part 2 demonstrates how Objectives 2, 3, and 4 are achieved using the model outputs.

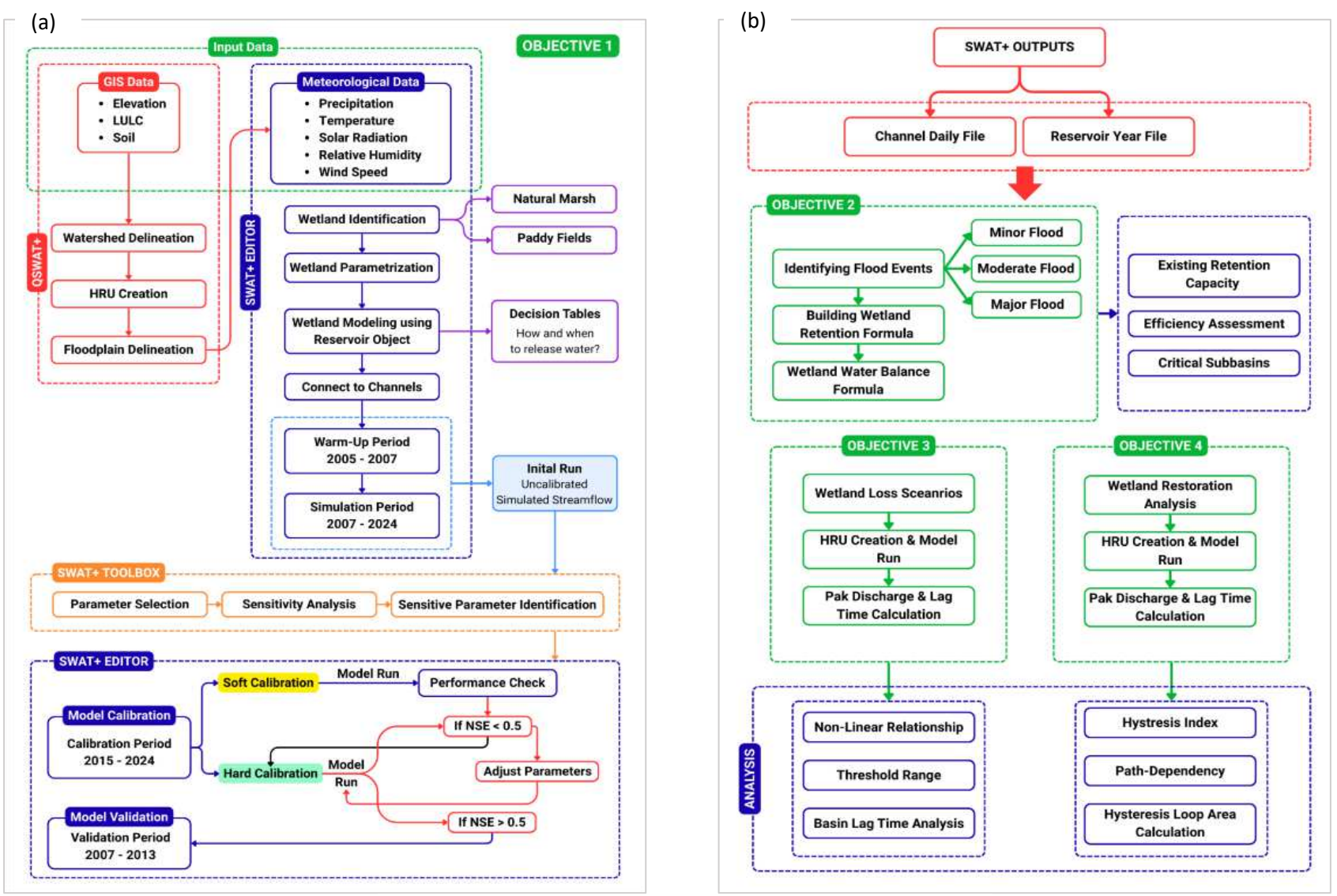


Figure 3: Research Methodology - (a) Part 1 (b) Part 2

3. RESULTS

3.1 Calibrated Hydrological Modelling Framework for Wetland Units

The QGIS interface of the SWAT+ (QSWAT+) was used to automate the hydrological discretization of the basin into 20 sub-basins. The main watershed outlet was manually defined at the Nagalagam Street gauging station. Based on the LULC layer, soil layer, and the topography layer, the watershed is further divided into unique set of Hydrological Response Units (HRUs), which are assumed to have a uniform hydrologic response. In SWAT+, floodplain delineation is integrated with HRUs to generate Landscape Units (LSUs). LSUs may represent a collection of HRUs within a subbasin, or distinct floodplain and upslope landscape positions. Three methods are available in SWAT+ for floodplain delineation: (i) Buffer Streams, (ii) DEM Inversion, and (iii) Branch Length. In this study, the floodplain was created by using the DEM Inversion method. This algorithm calculates a coefficient based on the topography to identify zones that may experience flooding during intensive rainfall periods. According to recent studies, this method provides a reliable representation of floodplains (Guilhen et al., 2022). The basin was discretized into 94 LSUs, specifically 47 upslope LSUs and 47 floodplain LSUs.

SWAT+ HRUs are unable to efficiently simulate wetland hydrology, as they are not connected to channels in a manner that allows for two-way flow, such as flooding and return flow. Furthermore, they are unable to model the overbank flow from rivers to the floodplain and cannot store large inundations. To overcome these limitations, SWAT+ offers the option of reservoir modelling, where wetlands can be modelled like reservoirs. Even though ecologically they are two distinct environments, the model allows wetlands to be represented in this way so that their key functions can be simulated within the model's computational structure (Armoa et al., 2024) (Figure 4). This allows water to flow back to the channel depending on both the wetland's storage capacity and the existing water volume. When the wetland is filled, water returns to the channel more quickly, whereas if it is not full, the flow is slower. To represent this, SWAT+ defines a principal and an emergency volume based on wetland depth and surface area. Wetland volume can decrease through losses such as seepage and evapotranspiration, and increase through inputs including rainfall, surface runoff, lateral flow from uplands, and overbank flow from the channel. Both natural marshes and paddy fields were modelled as reservoirs. For each marsh (293 HRUs) and paddy HRU (468 HRUs), surface area at principal and emergency spillway ($Area_{ps}$ and $Area_{es}$), and volume at principal and emergency spillway (Vol_{ps} and Vol_{es}) were calculated and imported to the SWAT+ Editor. Where:

$$Area_{ps} = HRU\ Area\ \times Fraction\ of\ HRU\ area\ at\ principal\ spillway \quad \text{Equation 1}$$

$$Area_{es} = HRU\ Area\ \times Fraction\ of\ HRU\ area\ at\ emergency\ spillway \quad \text{Equation 2}$$

$$Vol_{ps} = Area_{ps}\ \times Average\ depth\ of\ water\ at\ the\ principal\ spillway \quad \text{Equation 3}$$

$$Vol_{es} = Area_{es}\ \times Average\ depth\ of\ water\ at\ the\ emergency\ spillway \quad \text{Equation 4}$$

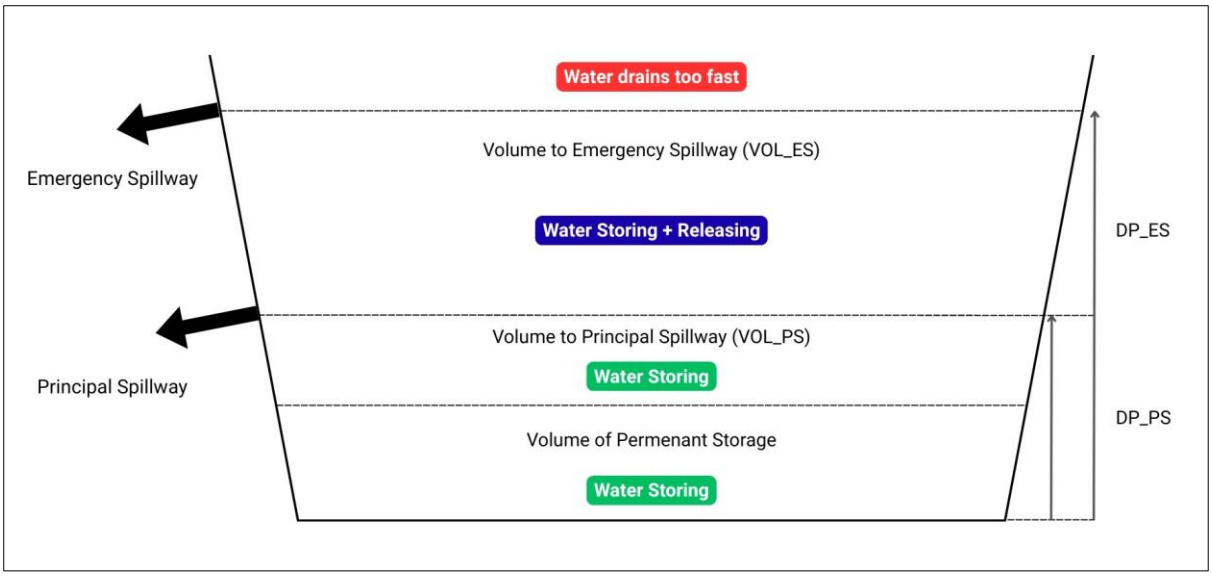


Figure 4: Wetland representation similar to the reservoirs in SWAT+

The Penman–Monteith method and the Muskingum method were used to simulate evapotranspiration and channel routing in the model, respectively. Table 2 shows the reservoir hydrology parameters used for marshes and paddy fields.

Table 2: Reservoir Hydrology Parameters for Marshes and Paddy Fields

SWAT+ Variable	Value for marshes	Value for Paddy fields	Description
HRU_PS	0.9	0.95	Fraction of HRU area at principal spillway
DP_PS	800 mm	100 mm	Average depth of water at the principal spillway
HRU_ES	1	1	Fraction of HRU area at emergency spillway
DP_ES	1500 mm	350 mm	Average depth of water at the emergency spillway
K	0.01 mm/hour	0.01 mm/hour	Hydraulic conductivity of the reservoir bottom
EVAP	0.7	0.6	Lake evaporation coefficient
VOL_AREA_CO	1	1	Volume-surface area coefficient for HRU impoundment
VOL_DP_A	1	1	Volume-depth coefficient for HRU impoundment
VOL_DP_B	1	1	Volume-depth coefficient for HRU impoundment
HRU_FRAC	1	1	Fraction of HRU that drains into impoundment

Sources: Armoa et al. (2024); Arnold et al. (2018)

Note: In the absence of site-specific local measurements, parameter values were estimated based on watershed and wetland area characteristics.

For paddy HRUs, the DP_PS is the standard agronomic depth for standing water in Sri Lankan paddy cultivation. DP_ES is the average height of a 'Niyara' (Bund). This acknowledges that while the crop might be damaged, the field physically holds this much water before spilling over.

Each wetland is then connected to the relevant outlet channel, through which it sends its outflow. A special feature of SWAT+ is the creation of decision tables, which allow users to determine how and when to release water. There are four sections in the decision tables of SWAT+: land use management, reservoir release, scenario land use, and flow conditions. For this study, the reservoir release decision table was used to input the wetland's water release commands. The model identifies the potential volume available for release ($V_{release}$) by comparing the existing water volume (V_i) against the volume at the principal spillway (V_{ps}) and the volume at the emergency spillway (V_{es}).

For the flow lag, the "days" option was selected. When the days option is selected, water release follows a drawdown schedule, meaning that any volume above the modeler-defined threshold will require "n" days to return to the channel. To simulate the recession of floodwater, the model calculates a threshold (T) using a release coefficient (C) (Arnold et al., 2018). There are various cases available in SWAT+ to calculate the volume of water released by wetlands using the file index (fp) option:

1. If the case "null" is used, the threshold for the reservoir is zero
2. If the case "pvol" is used, the threshold is calculated according to Equation 5

$$T = V_{ps} \times C$$

Equation 5

3. If the case is "evol" is used, the retention threshold is calculated according to Equation 6

$$T = V_{es} \times C$$

Equation 6

Finally, the release volume is calculated according to Equation 7.

$$V_{release} = \frac{V_S - T}{C}$$

Equation 7

Where V_S is the current water volume, T is the threshold value, and C is the release coefficient.

The model was configured with a two-year warm-up period, followed by a simulation period spanning from January 2005 to December 2024. To reduce the daily fluctuations and noise of the dataset, the daily streamflow was aggregated into monthly averages. The data were split into two sets: from 2015 to 2024 for calibration, and from 2007 to 2013 for validation. Table 3 shows the observations noted before the model calibration.

Table 3: Observations before Calibration

Simulated Condition	Reason	Considered Significant Parameters
High surface runoff ratio (>0.8)	Too much rainfall becomes runoff	• Curve Number (CN2) • Soil Evaporation Compensation Factor (ESCO) • Maximum Canopy Storage (CANMX) • Percolation Coefficient (PERCO)

The model overestimates the flow (High Flow Peaks)	Runoff is too high/ Excess surface flow	• Potential Evapotranspiration Coefficient (PETCO) • Curve Number 3 Soil Water Factor (CN3_SWF) • Lateral Soil Flow Coefficient (LATQ_CO) • Soil Available Water Capacity (AWC) • Saturated Hydraulic Conductivity (K) • ESCO • Surface runoff lag time (SURLAG) • Manning's N for Channel (CH_N) • Plant Uptake Compensation Factor (EPCO) • Floodplain Roughness Coefficient Number (FPN)
Low Baseflow	Groundwater contribution underestimation	• PERCO • Baseflow Alpha Factor (ALPHA) • Threshold depth of water in the shallow aquifer (REVAPMN) • Groundwater Revap coefficient (REVAP_CO)

SWAT+ soft calibration method was used in the first round of calibration, which requires 10 – 12 simulations following a one-at-a-time procedure. Once the soft calibration is complete, the hard calibration only requires minor adjustments to the peaks and recessions. Then, to identify the most sensitive parameters, a sensitivity analysis was conducted using the Latin Hypercube - One Factor at a time (LH-OAT) method in the SWAT+ Toolbox. Sixteen parameters were evaluated using 100 samples, resulting in a total of 1700 simulations (calculated as N×(P+1), where N = 100 and P = 16). The performance of the model was insufficient with the soft calibration with NSE (Nash-Sutcliffe Efficiency) value less than 0.29. Table 4 shows the first-order sensitivity values for each parameter, after 1700 model runs. The parameters that received 0 or nearly 0 values are considered low-sensitivity parameters for the study.

Table 4 - First Order Sensitivity of the Parameters

Parameter	**Full Name**	**Unit**	**1st Order Sensitivity**
CN2	SCS Curve Number (Moisture Condition II)	–	0.870935985
CANMX	Maximum Canopy Storage	mm H_2O	0.562075924
CN3_SWF	Curve Number Adjustment Factor for Soil Water	–	0.517781365
PERCO	Percolation Coefficient	–	0.461834597
LATQ_CO	Lateral Flow Coefficient	–	0.364241661
ESCO	Soil Evaporation Compensation Factor	–	0.125273715
PETCO	Plant Evapotranspiration Compensation Factor	–	0.108990912
AWC	Available Water Capacity	mm H_2O / mm soil	0.042270061
K	Hydraulic Conductivity (Soil)	mm/hr	0.024085642
ALPHA	Baseflow Alpha Factor	1/day	0.014045944
REVAPMN	Threshold Water Depth for Revaporation	mm H_2O	0.004086789
CH_N	Manning's Roughness Coefficient for Main Channel	–	0.00213361
EPCO	Plant Uptake Compensation Factor	–	0
FPN	Floodplain Manning's Roughness Coefficient	–	0
REVAP_CO	Revaporation Coefficient	–	0
SURLAG	Surface Runoff Lag Coefficient	–	0

The hard calibration was performed using the significant parameters identified through the sensitivity analysis. Parameter values were adjusted within their predefined minimum and maximum bounds using a selective parameter modification approach. Parameter adjustments were implemented using either percentage change (pctchg), whereby the existing parameter value is modified by a specified percentage, or absolute value

replacement (absval), where the parameter is directly assigned a new value within the defined range. Table 5 presents the change types, minimum and maximum parameter ranges, and the optimal values of the sensitive parameters.

Table 5: Significant parameters and their optimal values

Parameter	Change Type	Minimum	Maximum	Optimal Value
CN2	pctchg	35	95	-35
CANMX	absval	0	100	99
ESCO	absval	0	1	1
PETCO	absval	0.8	1.2	1.18
PERCO	absval	0	1	0.24
CN3_SWF	absval	0	1	0.3
LATQ_CO	absval	0	1	0.15

Figure 5 illustrates the comparison between observed and simulated streamflow after calibration. The model was validated for the period 2007–2014 using the calibrated parameter set. Figure 6 illustrates the observed and simulated streamflow during validation. Table 6 presents the corresponding model performance metrics for both calibrated and validated models. The final model performance metrics indicate that overall performance ranges from satisfactory to good during both the calibration and validation periods, suggesting that the model adequately represents watershed hydrological processes.

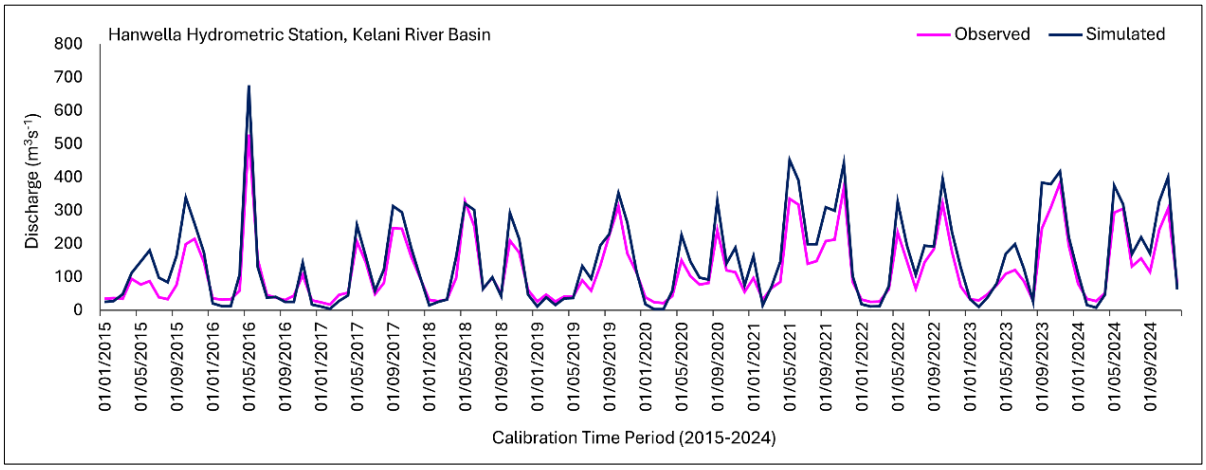


Figure 5: Observed Vs Simulated Flow of the calibrated model

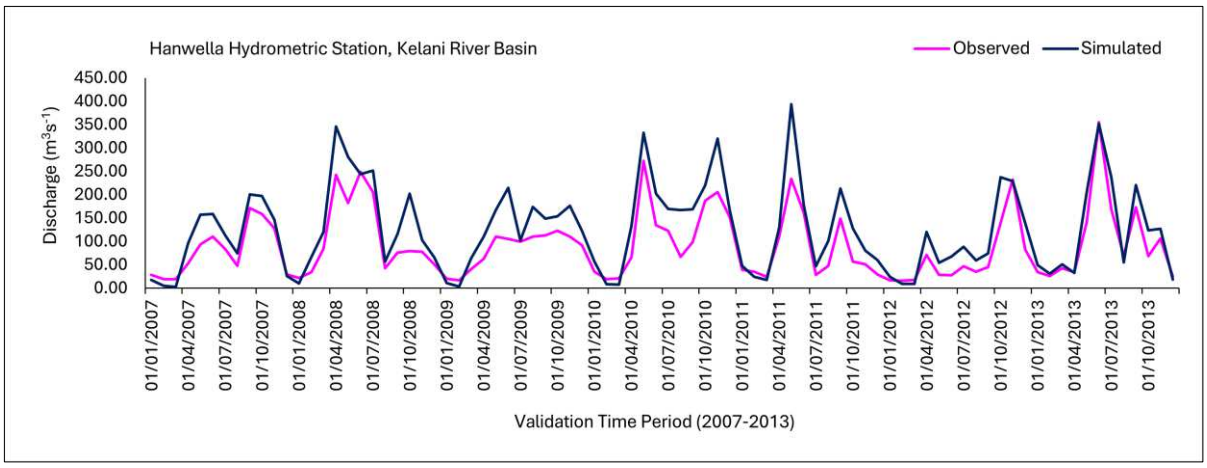


Figure 6 - Observed Vs. Simulated Flow of the validated model

Table 6: Performance of the calibrated and validated models

Metric	Equation	Model	Value	Performance
NSE	$NSE = 1 - \frac{\sum_{t=1}^{n}(O_t - S_t)^2}{\sum_{t=1}^{n}(O_t - \bar{O})^2}$ Equation 8 (Nash & Sutcliffe, 1970) O_t: Observed value at time t S_t: Simulated value at time t	Calibrated	0.75	Very Good
	>0.75 Very Good 0.65– 0.75 Good 0.5 – 0.65 Satisfactory <0.5 Unsatisfactory	Validated	0.53	Satisfactory
PBIAS	$PBIAS = 100 \times \frac{\sum_{t=1}^{n}(S_t - O_t)}{\sum_{t=1}^{n} O_t}$ Equation 9 (Moriasi, et.al., 2007)	Calibrated	-24.67	Satisfactory
	±0–10% Very Good ±10–15% Good ±15–25% Satisfactory >±25% Unsatisfactory	Validated	-37.28	Unsatisfactory
KGE	$KGE = 1 - \sqrt{(r-1)^2 + (\beta-1)^2 + (\gamma-1)^2}$ Equation 10 (Gupta, et.al., 1999) where r = correlation, β =bias ratio, $\gamma = \frac{CV_S}{CV_O}$, *where* CV_S = Coefficient of variation of simulated flow, CV_O = Coefficient of variation of observed flow	Calibrated	0.936	Very Good
	>0.75 Very Good 0.65 – 0.75 Good 0.5 – 0.65 Satisfactory <0.5 Unsatisfactory	Validated	0.863	Very Good

$R^2 = \frac{[\sum_{t=1}^{n}(O_t - \bar{O})(S_t - \bar{S})]^2}{\sum_{t=1}^{n}(O_t - \bar{O})^2 \cdot \sum_{t=1}^{n}(S_t - \bar{S})^2}$ Equation 11 (Chu & Shirmohammadi, 2004; Singh, et.al., 2005) R^2 $\bar{O}, \bar{S}$: Mean of observed and simulated values, respectively		Calibrated	0.946	Very Good
		Validated	0.878	Very Good

0.7–1.0	Very Good
0.4–0.7	Satisfactory Good
<0.4	Unsatisfactory

3.2 Subbasin-Scale Wetland Retention Capacity under Extreme Rainfall

To evaluate wetland resilience under extreme hydrological conditions, a representative "Major Flood" was defined statistically using the Log-Pearson Type III (LP3) distribution method (England et al., 2018), considering its flexibility in fitting skewed hydrological data (Equation 12). This was applied to the 20-year historical streamflow data (2005–2024) simulated by the calibrated SWAT+ model to identify discharge levels related to specific Annual Exceedance Probabilities (AEP).

$$Q_t = 10 \text{ ^ } (\bar{y} + K_t \cdot S_Y)$$

Equation 12

where Q_t is the maximum discharge for return period t, $\bar{y}$ is the mean of $\log_{10}$ (annual peak discharge), S_y is the standard deviation, and K_t is the frequency factor. The calculated Q_t corresponded to the May 2016 flood event associated with Cyclone Roanu, characterized by continuous rainfall exceeding 300 mm over three days in the upper catchment.

This event was validated against observed streamflow records from the Irrigation Department (Figure 7).

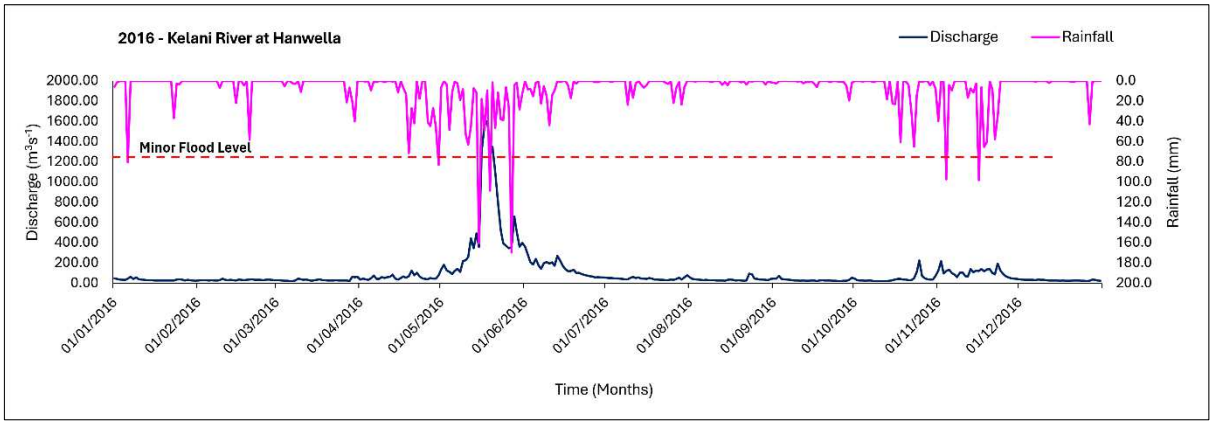


Figure 7: Discharge and Rainfall for 2016, Kelani River at Hanwella River Gauge

The model was run using 2016 weather data to quantify the retention capacity of the wetland environments. This study defines water retention capacity as the ability of a landscape to capture, store, and slow down precipitation, thus preventing immediate surface runoff and flood peaks (Chow,1964). The maximum retention volume of

wetland environments ($V_{retention}$) was calculated by aggregating storage capacities of marshes and paddy fields, accounting for their distinct hydrological characteristics (Equation 13).

$$V_{retention} = \sum[(A_{marsh} \times D_{marsh}) - V_{marsh_initial}] + [(A_{paddy} \times D_{paddy}) - V_{paddy_initial}]$$

Equation 13

where A represents the area of the Natural Marsh or Paddy Field within the sub-basin (m^2), D is the maximum inundation depth that the landscape can sustain (This is 1.5m for marshes & 0.35m for paddy fields based on local hydraulic characteristics), and $V_{initial}$ is principal spillway volume of paddy fields and marshes. The retention deficit ($V_{deficit}$) was calculated when wetland capacity was insufficient, which is the difference between total volume of water entering the wetland system and the volume that could be retained within its storage capacity. The net volume entering wetland (V_{enter}) follows the water balance equation (Armoa, et.al., 2024) (Equation 14).

$$V_{enter} = V_{in} - V_{out} + V_{return}$$

Equation 14

where V_{in} = Total inflow coming to the wetland; this includes precipitation, surface runoff, and the lateral flow from upland (obtained from the reservoir_year output file).

V_{out} = Total outflow or release from the wetland; this includes evapotranspiration and seepage (obtained from the reservoir_year output file).

V_{return} = Overbank flow coming from the channels, calculated using Manning's equation for bank full discharge.

Table 7 shows the overall retention capacity of the basin under major flood condition. As shown in Figure 8 and Table 8, the most inundations were concentrated in the lower basin, specifically in subbasins 4, 6, 8, 10, 16, 17, and 18. Notably, these sub-basins include 42% of the total wetland area within the watershed. Retention efficiencies of wetland environments were further assessed for two additional types of flood events (minor and moderate floods), specifically for the identified critical subbasins mentioned above (Table 9).

Table 7 - Basin-Scale Retention Capacity Assessment Under Major Flood Conditions

Component	**Value**	**Unit**
Total Marsh Area	45.2	km^2
Total Paddy Area	177.4	km^2
Marsh Retention Capacity	680×10^5	m^3
Paddy Retention Capacity	621×10^5	m^3
Total Retention Capacity ($V_{retention}$)	$1{,}300 \times 10^5$	m^3
Total Volume Entering Wetlands V_{enter}	$1{,}510 \times 10^5$	m^3
Total Retention Deficit ($V_{deficit}$)	210×10^5	m^3
Basin-Wide Average Retention Efficiency	40.3	%

1 Table 8: Simulated excess flow during 2016 flood

Subbasin	Total Excess Flow on Flood Days (m^3)	Wetland Area (Sq.km)
1	945.46	24.70
2	718.93	8.72
3	502.76	3.68
4	1,027.52	13.05
5	462.15	4.46
6	17,143.91	12.47
7	669.19	10.87
8	20,262.40	19.49
9	1453.24	1.94
10	4,890.43	19.95
11	1,219.76	0.95
12	543.66	2.99
13	599.22	3.21
14	829.02	6.40
15	722.71	0.88
16	1,590.21	24.44
17	33,015.00	18.69
18	36,646.60	23.29
19	592.43	2.44
20	901.37	19.35

2

3 Table 9: Retention efficiencies for different flood types

Subbasin	Wetland Area (km^2)	Retention Efficiency		
		Type A - Minor Flood (150-200mm) Return Period - 1-2 Yrs	Type B - Moderate Flood (200-300mm) Return Period - 2-5 Yrs	Type C - Major Flood (>300mm / 2016 Event) Return Period - >20 Yrs
4	13.05	26.30%	23.20%	20.16%
6	12.47	32.10%	28.40%	24.65%
8	19.49	30.60%	27.00%	23.46%

10	19.95	37.70%	33.40%	29.04%
16	24.44	33.20%	29.30%	25.45%
17	18.69	30.40%	26.90%	23.37%
18	23.29	34.70%	30.70%	26.68%

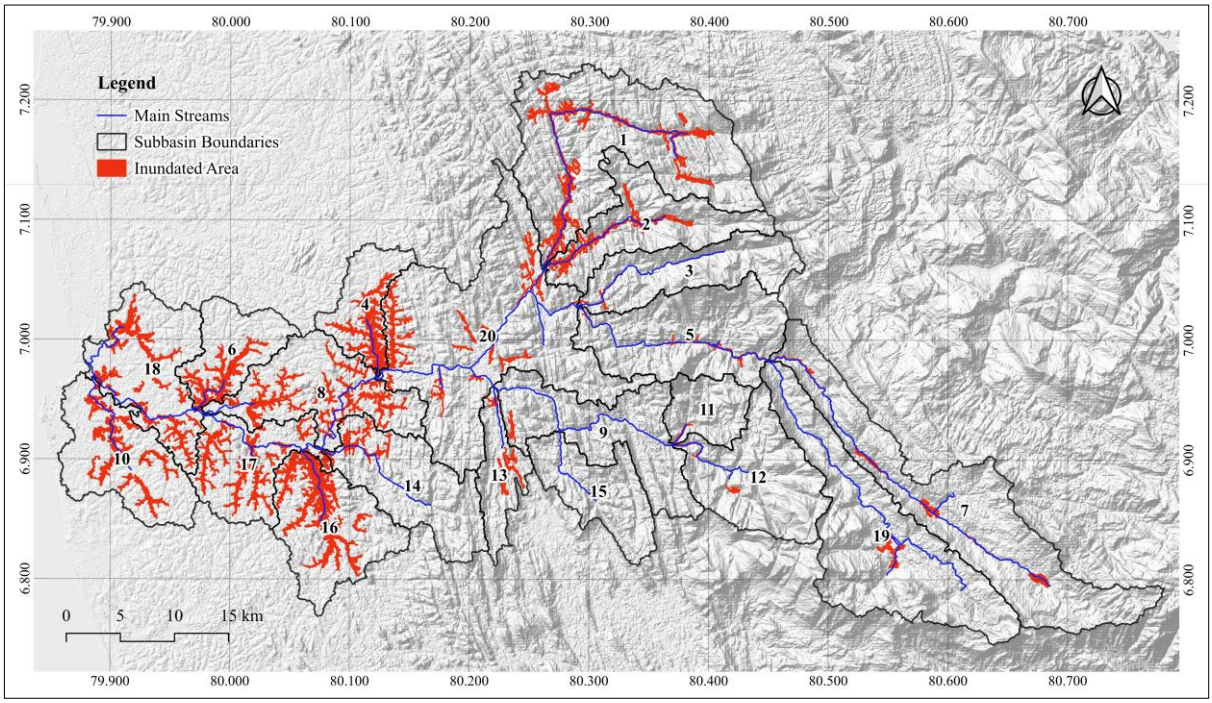


Figure 8: Inundated areas during the 2016 flood event derived from Sentinel-1 SAR imagery

3.3 Nonlinear Basin Response to Progressive Wetland Loss (5–90%)

To quantify the nonlinear hydrological response of the basin to wetland loss, a series of scenarios was created. These scenarios were developed by gradually reducing the areas of natural marshes and paddy fields from the initial LULC (Figure 9), according to a rule-based spatial prioritization approach reflecting realistic urban expansion patterns (Appendix A). In each scenario, the target percentage of wetland environment loss was converted to the built-up class.

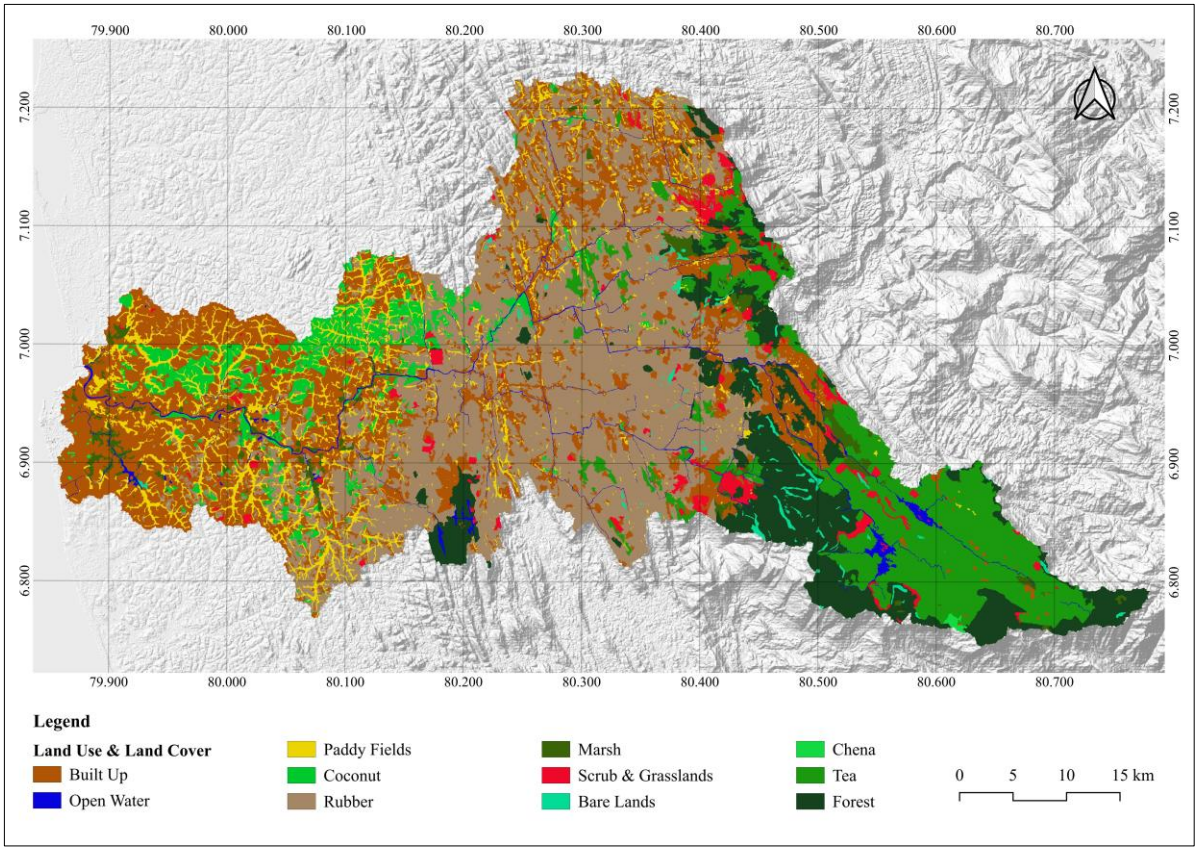


Figure 9: LULC Classification for the Kelani River Basin

All simulations were performed from January 2024 to December 2024, using rainfall and other meteorological data from the identified flood event (2016), ensuring that the simulated soil moisture and evapotranspiration rates reflect the actual atmospheric conditions associated with the critical flood period. For each scenario, the watershed was discretized into HRUs representing the altered LULC. For each scenario, the HRUs classified as marsh and paddy were parametrized as reservoir objects in the editor and hydraulically linked to the relevant subbasin channel.

To assess the non-linear relationship between wetland loss and its hydrological impact, peak discharge (Q_{peak}) and lag time (t_{lag}) were calculated for each scenario. For each scenario, peak discharge was obtained from the channel_sd_day output file, and lag time was calculated using Equation 15.

$$t_{lag} = t_{Q_peak} - t_{p_centroid}$$

Equation 15

Where t_{Q_peak} is the time index (day) when the river discharge reached its maximum value and $t_{p_centroid}$ is the time index (day) of the center of mass of the rainfall storm. $t_{p_centroid}$ was calculated using Equation 16, where P_i is the daily rainfall depth, t_i is the time index relative to the storm onset, and n is the duration of the storm event in days.

$$t_{p_centroid} = \frac{\sum_{i=1}^{n}(P_i - t_i)}{\sum_{i=1}^{n} P_i}$$

Equation 16

The timing of peak discharge (t_{Q_peak}) was computed using Equation 17, where D_{max} is the day index corresponding to the maximum simulated flow, and δ is an adjustment factor introduced to refine the peak timing within the daily time step.

$$t_{Q_peak} = D_{max} + \delta$$

Equation 17

The adjustment factor (δ) was assigned based on the position of the hydrograph peak within the day as follows:

- δ = 0.0 when the peak is distinctly centered within the identified day
- δ = -0.2 when the peak occurs early (shifted toward the previous day)
- δ =+0.8 when the peak occurs late, (shifted toward next day)
- δ = 0.5 when the peak is symmetrically distributed within the daily interval

Table 10 shows the obtained outputs for each wetland loss scenario.

Table 10: Wetland Loss Scenario Analysis

Scenario	**Loss %**	**Peak Discharge (Q_{peak}) [m^3/s]**	**Time Peak (t_{Q_peak}) [Days]**	**Lag Time (t_{lag}) [Days]**	**Change from Baseline**
Baseline	0%	1,604	6	2.54	0
Scenario 1	5%	1,620	6	2.54	+1%
Scenario 2	10%	1,645	6	2.54	+2.6%
Scenario 3	15%	1,680	6	2.54	+4.7%
Scenario 4	20%	1,725	6	2.54	+7.5%
Scenario 5	25%	1,790	5.8	2.34	+11.6%
Scenario 6	30%	1,870	5.8	2.34	+16.6%
Scenario 7	35%	1,960	5.8	2.34	+22.2%
Scenario 8	40%	2,060	5.5	2.04	+28.4%
Scenario 9	45%	2,170	5.5	2.04	+35.3%
Scenario 10	50%	2,290	5.5	2.04	+42.8%
Scenario 11	60%	2,550	5.2	1.74	+59%
Scenario 12	70%	2,820	5	1.54	+75.8%
Scenario 13	80%	3,100	5	1.54	+93.3%
Scenario 14	90%	3,350	4.8	1.34	+108.9%
Total Change	**90%**	**+1746**	**-1.2**	**-1.2**	**+108.9%**

As shown in the Table 11, the time to peak is reduced by 6 to 4.8 days, meaning the lag time decreases by 1.2 days (47% reduction). At maximum wetland loss (90%), the basin will generate peak flows approximately 29 hours earlier than baseline conditions (Figure 10). This reduction in warning time, combined with the 109% increase in peak discharge, will severely compromise emergency response capabilities.

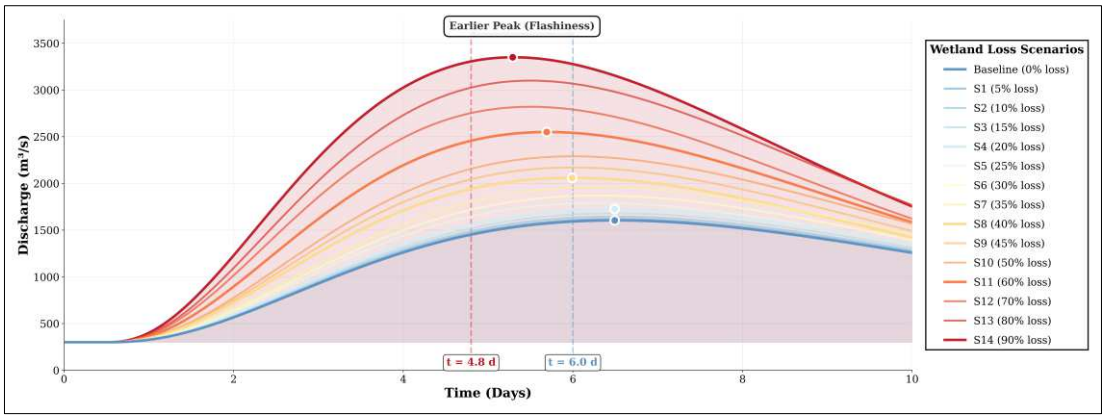


Figure 10: Comparative Hydrographs under Wetland Loss Scenarios

To evaluate the relationship between wetland loss and peak discharge, linear, quadratic (polynomial), and exponential regression models were fitted to the simulated data. Model performance was evaluated using the coefficient of determination (R^2) and the Root Mean Square Error (RMSE). The optimal model was selected according to the highest R^2 value and the lowest RMSE (Table 11). The polynomial model demonstrated the best fit compared to the linear model. The positive coefficient of the quadratic term (a = 0.15) confirms an accelerating relationship, indicating that each additional percentage of wetland loss produces a progressively larger increase in peak discharge (Figure 11).

Table 11: Comparative Performance of Regression Models Describing the Relationship Between Wetland Loss and Peak Discharge

Model	Equation	R^2 Value	RMSE (m^3/s)
Linear	$Q_{peak} = 20.1(L\%) + 1379$	0.957	118.2
Polynomial	$Q_{peak} = 0.15(L\%)^2 + 6.18(L\%) + 1567$	0.997	38.7
Exponential	$Q_{peak} = 689.3 \times e^{(0.0146 \times L\%)} + 843$	0.994	62.4

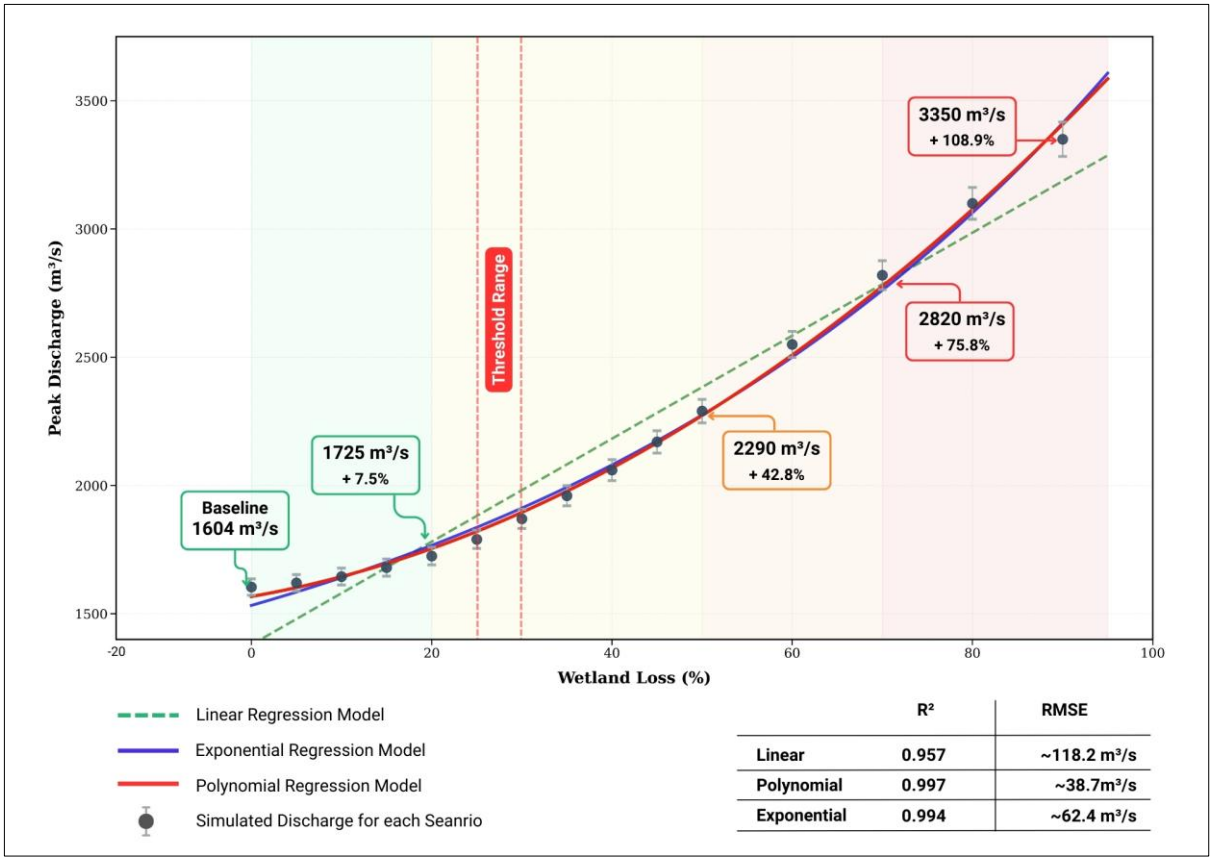


Figure 11: Non-Linear Curve: Wetland Loss Vs. Peak Discharge

3.4 Hysteresis Dynamics and System Memory Response Under Incremental Wetland Restoration

To assess the hysteresis and path dependency response of the watershed, a series of wetland restoration scenarios was created. Restoration scenarios followed hydrologically informed spatial criteria, prioritizing low-lying areas, stream-adjacent zones, and locations suitable for connectivity enhancement while excluding urban cores and prime agricultural lands (Appendix B). When wetlands are intentionally restored, natural ecosystems are created for maximum ecological benefits. Since paddy fields are agricultural systems that function as wetlands, for the gain scenarios, only natural marsh restoration was considered, while paddy field areas remained unchanged as the initial LULC. This asymmetric treatment of wetland types is that the international conservation and restoration frameworks, including guidance under the Ramsar Convention on Wetlands, primarily emphasize the protection and restoration of natural marsh ecosystems rather than the expansion of agricultural wetlands. Furthermore, paddy fields represent transitional land uses within rapidly urbanizing watersheds; although they may be converted into built-up areas, they are rarely targeted as restoration end-states. Consequently, distinguishing between natural marsh restoration and agricultural wetland persistence allows for a more realistic representation of ecological restoration pathways and watershed memory behavior. Since wetland restoration cannot be conducted on steeper slopes or in dense urban areas, the land use suitability was considered when creating the LULC maps used in this model (Table 12). Table 13 shows the obtained outputs for each wetland restoration scenario.

Table 12: Potential areas for wetland restoration

Consideration	Potentials
Land Use & Land Cover	Scrub/Grasslands, Bare Lands, Chena, and areas near Water bodies, adjacent areas to paddy fields were considered as the most feasible locations for restoration.
	Urban and Forest areas were excluded.
Slope	Only areas with a slope of < 5% were considered. Wetlands require depression storage and flat terrain to retain water.
Soil	Study area is characterized only by the soil groups under hydrological category C, which is the soil group found in wetlands. Therefore, soil group was not specifically considered in creating the LULC layers.

Table 13: Wetland Restoration Scenario Analysis

Scenario	Restoration %	Peak Discharge (Q_{peak}) [m^3/s]	Time Peak (t_{Q_peak}) [Days]	Lag Time (t_{lag}) [Days]	Change from Baseline
Baseline	0%	1,604	6	2.54	0
Scenario 1	5%	1,520	6	2.54	-5.2%
Scenario 2	10%	1,455	6.2	2.74	-9.3%
Scenario 3	15%	1,395	6.2	2.74	-13%
Scenario 4	20%	1,340	6.2	2.74	-16.5%
Scenario 5	25%	1,290	6.5	3.04	-19.6%
Scenario 6	30%	1,245	6.5	3.04	-22.4%
Scenario 7	35%	1,205	6.5	3.04	-24.9%
Scenario 8	40%	1,170	6.8	3.34	-27.1%
Scenario 9	45%	1,140	6.8	3.34	-28.9%
Scenario 10	50%	1,115	6.8	3.34	-30.5%
Scenario 11	60%	1,075	7	3.54	-33%
Scenario 12	70%	1,045	7	3.54	-34.8%
Scenario 13	80%	1,025	7.2	3.74	-36.1%
Scenario 14	90%	1,010	7.2	3.74	-37%
Total Change	**90%**	**-594**	**1.2**	**1.2**	**-37%**

Hysteresis analysis was conducted by comparing the response pathways of wetland loss and restoration scenarios. The hysteresis index (HI) was calculated as the normalized difference between loss impact and restoration benefit at equivalent scenario intensities (Equation 15), where HI = 0 means no hysteresis (symmetric response), HI > 0 means positive hysteresis (loss > restoration) and HI = 1 means complete hysteresis (no recovery possible).

$$Hysteresis\ Index\ (HI) = \frac{\left|\Delta Q_{peak_loss}\right| - \left|\Delta Q_{peak_restoration}\right|}{\left|\Delta Q_{peak_loss}\right|}$$

Equation 18

Table 14 shows the results of the HI calculation. Accordingly, at 90% scenario, wetland loss increased peak discharge by 1,746 m³/s (+109%), while equivalent restoration reduced it by only 594 m³/s (-37%), indicating a hysteresis index of 0.66. This indicates that only 34% of flood attenuation capacity lost through wetland degradation can be recovered through equivalent restoration efforts.

Table 14: Hysteresis Index Calculation

Scenario (%)	Q_{peak_loss}	$Q_{peak_restoration}$	ΔQ_{peak_loss}	$\Delta Q_{peak_restoration}$	HI
5	1,620	1,520	16	84	-4.25
10	1,645	1,455	41	149	-2.63415
15	1,680	1,395	76	209	-1.75
20	1,725	1,340	121	264	-1.18182
25	1,790	1,290	186	314	-0.68817
30	1,870	1,245	266	359	-0.34962
35	1,960	1,205	356	399	-0.12079
40	2,060	1,170	456	434	0.048246
45	2,170	1,140	566	464	0.180212
50	2,290	1,115	686	489	0.287172
60	2,550	1,075	946	529	0.440803
70	2,820	1,045	1,216	559	0.540296
80	3,100	1,025	1,496	579	0.612968
90	3,350	1,010	1,746	594	0.659794

Five clear path scenarios were developed to study the impact of historical wetland alteration pathways on final hydrologic outcomes (Table 15). Each path started at baseline conditions and underwent a sequence of wetland loss and equivalent wetland restoration.

Table 15: Peak Discharge Response Under Sequential Wetland Loss–Restoration Pathways and Deviation from Baseline Conditions

Pathway	**Sequence**	**Post-Loss Q_{peak} ($Q_{degraded}$)**	**Post-Restoration Q_{peak} (Q_{final})**	**Deviation from Baseline**
A	0% → 0%	1,604 m³/s	1,604 m³/s	0%
B	0% → 25% Loss → 25% Restoration	1,790 m³/s	1,476 m³/s	-8.00%
C	0% → 50% Loss → 50% Restoration	2,290 m³/s	1,801 m³/s	+12.30%
D	0% → 70% Loss → 70% Restoration	2,820 m³/s	2,261 m³/s	+41.00%
E	0% → 90% Loss → 90% Restoration	3,350 m³/s	2,756 m³/s	+71.80%

At low levels of degradation, the basin shows a compensatory response. For the B-sequence, Q_{final} (1,476 m³/s) was about 8% lower than the baseline. This result is explained by the imbalance between the impact of degradation and restoration at low intensities: the decrease in flow due to restoration (-314 m³/s at 25%) was greater than the increase in degradation (+186 m³/s at 25%). This suggests that in systems with low degradation, restoration can

lead to a net hydrological state similar to or slightly better than the initial state. However, even when similar restoration measures were applied under moderate to high levels of degradation, the basin did not fully recover to its initial conditions (paths C/D/E). The final flow remained stable above the baseline, and with the intensity of degradation, the magnitude of this residual effect increased (Figure 12).

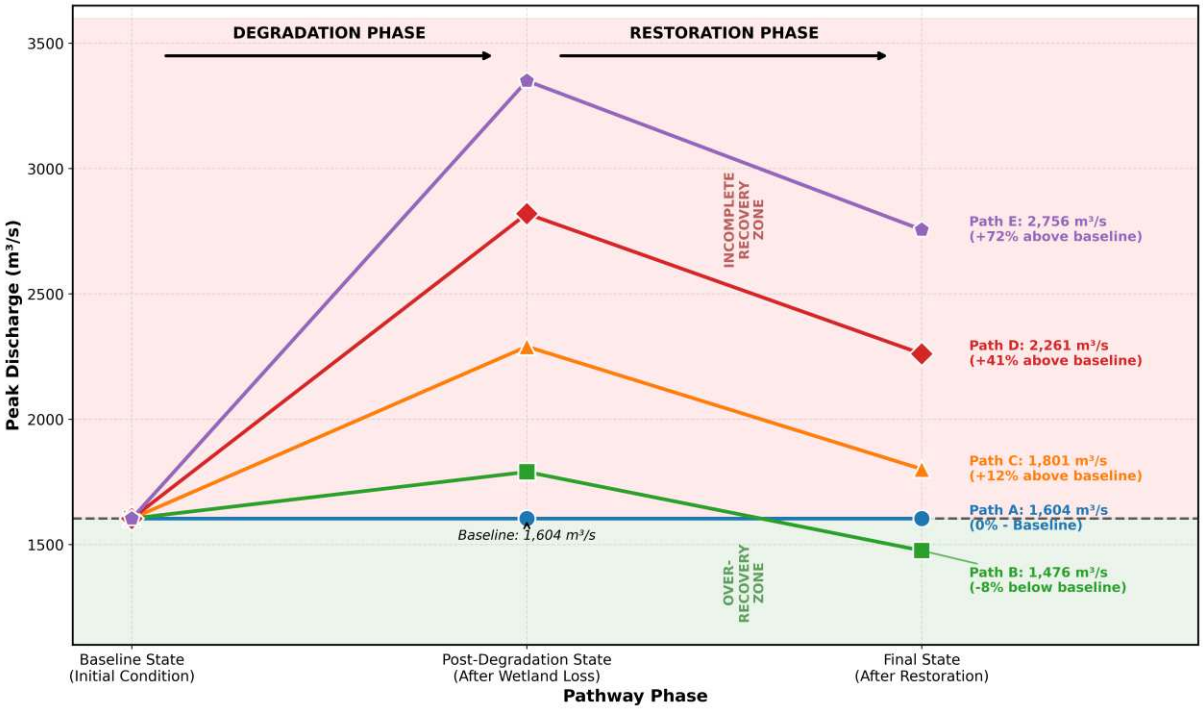


Figure 12: Path dependency in peak discharge response under sequential wetland degradation and restoration scenarios.

The cumulative asymmetry between degradation and restoration is quantified by the hysteresis loop area. It represents the total hydrological deficit that cannot be recovered even through restoration efforts of equal magnitude. This loop area is calculated using the trapezoidal rule. For each interval of wetland change, the area under the degradation and restoration curves was calculated (Equation 19), where, Y_1 and Y_2 represent the peak discharge values at the beginning and end of the interval, respectively, and Δx denotes the percentage change in wetland extent over that interval.

$$Area = \frac{Y_1 + Y_2}{2} \times \Delta x$$

Equation 19

The hysteresis loop area for each interval was then computed as the difference between the degradation and restoration areas, and the total hysteresis loop area was obtained by summing these interval-wise differences (Table 16). As illustrated in Figure 13, the shaded region between the degradation and restoration curves visually represents the cumulative hysteresis loop area.

Table 16: Hysteresis Loop Area Calculation

Interval	Loss Area	Restoration Area	Loop Area
0-25%	42,425	36,175	6,250
25-50%	51,000	30,063	20,937

50-70%	51,100	21,600	29,500
70-90%	61,700	20,550	41,150
Total	**206,225**	**108,388**	**97,837**

To provide a normalized measure of system irreversibility, the Normalized Hysteresis Area Index (NHAI) was calculated (Equation 20).

$$NHAI = \frac{Total\ Loop\ Area}{Total\ Loss\ Area} \times 100\% \quad \text{Equation 20}$$

The computed NHAI value of 47.4% indicates that nearly half of the cumulative hydrological impact generated during wetland degradation cannot be offset by equivalent restoration efforts.

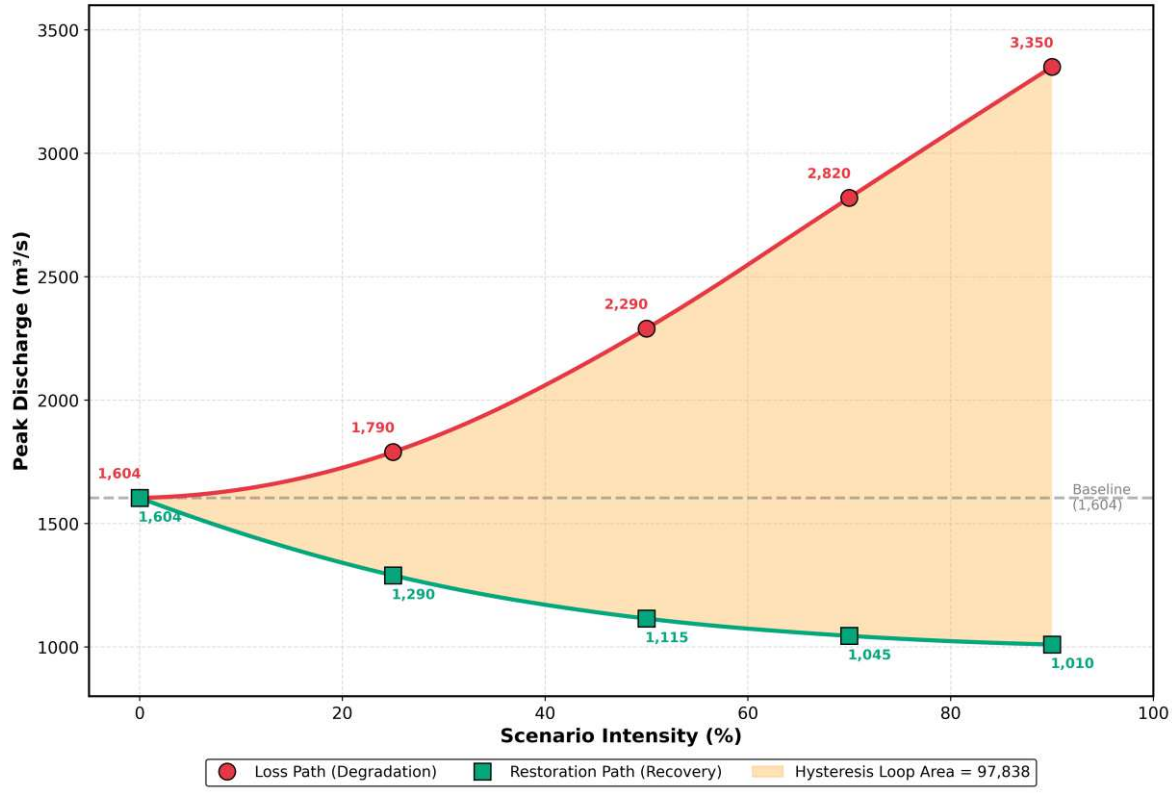


Figure 13: Hysteresis loop area between degradation and restoration trajectories of peak discharge, corresponding to an NHAI of 47.4%

4. DISCUSSION

This study addressed critical gaps in wetland hydrology research by moving beyond simplified "with–without wetland" comparisons and instead examining the cumulative, incremental effects of wetland degradation and restoration within a Complex Adaptive System (CAS) framework. By focusing specifically on progressive wetland loss and recovery in the Kelani River Basin, the research contributes new empirical evidence on nonlinear

hydrological behaviour, threshold dynamics, and system memory dimensions that remain insufficiently explored in existing watershed-scale studies.

4.1 Differentiating Natural and Management Wetlands in Hydrological Modelling Framework

Several studies in wetland hydrology have demonstrated that wetlands provide significant flood control and streamflow regulation services, particularly through the application of hydrological modelling approaches (Kumar, etal., 2021; e Sousa & Miranda, 2018; Mitsch & Gosselink, 2015; Acreman & Holden, 2013; Wen et al., 2013; Padmanabhan & Bengtson 2001). However, most watershed-scale modelling frameworks and ecosystem service assessments continue to represent wetlands as a homogeneous class, without explicitly distinguishing between natural wetlands and managed systems such as paddy fields when evaluating flood mitigation functions (Mukherjee et al., 2021). In many parts of Sri Lanka and across Asia, paddy fields operate as incidental or managed wetlands, playing a critical role in flood attenuation, baseflow regulation, and groundwater recharge (Kudo et al., 2015). Although process-based models have been developed to simulate paddy water management, irrigation dynamics, and nutrient transport (Zhang, et al., 2025; Xia et al., 2022, Kamruzzaman, et al., 2020), the combined and distinct contributions of natural and managed wetland types to nonlinear flood regulation processes remain inadequately explored in the existing literature.

Therefore, the first objective of this study was to develop and calibrate a hydrological modelling framework that distinguishes natural marshes and paddy fields as separate yet functionally interconnected hydrological units. Using SWAT+, wetlands were explicitly represented as storage reservoirs within watershed routing structure with parameters values applied separately for natural marshes and managed paddy systems. The calibrated model demonstrated satisfactory to very good performance across NSE, KGE, and R^2 metrics, confirming that the framework reliably captures watershed-scale hydrological processes.

4.2 Sub-Basin Scale Wetland Retention Capacity and Storage Deficit under Extreme Events

Previous studies have established that wetlands provide important flood attenuation services but emphasize that their effectiveness is constrained by finite storage capacity and event magnitude (Acreman & Holden, 2013; Bullock & Acreman, 2003). However, most existing assessments rely on simplified binary representations of wetlands or do not explicitly quantify the relationship between storage capacity and incoming flood volumes at the watershed scale (Opperman et al., 2009; Dadson et al., 2017). The second objective of this study addresses this gap by providing a sub-basin scale quantification of wetland retention capacity and identifying a measurable retention deficit under extreme rainfall conditions.

Results show that wetlands in the Kelani Basin collectively provide approximately $1{,}300 \times 10^5$ m³ of storage during major flood events (<300 mm rainfall) yet an annual retention deficit of 210×10^5 m³ (≈16% of total capacity) already exists under present conditions. Natural marshes demonstrated particularly high storage efficiency per unit area, providing approximately 2.5 times more flood storage per hectare than rice paddies. The retention efficiency ranges at 18% to 34% during identified several flood events and the lower basin areas are already stressed, indicating higher retention deficits and excess flows during flood events. Sub-basins 4, 6, 8, 10, 16, 17 and 18 showed the highest excess flows and significant retention deficits during the major flood event. These sub-basins, which include 42% of the basin's wetland area and provide 58.7% of the total retention capacity, remain flood-prone areas, as upstream water accumulates faster than the local wetlands can accommodate. The

retention efficiency of these critical sub-basins is found to be 20% to 29% during major floods, 23% to 33% during moderate floods, and 26% to 38% during minor floods. This confirms that even in small or frequent events, wetlands cannot fully or partially capture the flood volumes received. Paddy Fields collectively hold almost half of the total storage capacity across their vast area. Although flood attenuations services in paddy fields are incidental to their agricultural use, it is a valuable ecosystem service that should be recognized and conserved.

4.3 Threshold Behaviour and Nonlinear Hydrological Response to Progressive Wetland Loss

Numerous studies have demonstrated that hydrological systems exhibit nonlinear responses to land-use change and climate variability (Zehe & Sivapalan, 2009; Vreugdenhil et al., 2022). In the context of deforestation, urbanization, and broader land-cover transitions, threshold-like behavior and asymmetric changes in runoff generation and water storage have been widely reported (Gentine et al., 2012; Lopes et al., 2022). However, such nonlinear dynamics are rarely examined in relation to wetland loss in isolation. Instead, wetlands are typically treated as a single land-cover category within broader modelling frameworks, without explicitly assessing how incremental reductions in wetland extent influence flood peaks and runoff volumes (Jing et al., 2025)

The third objective of this study investigates nonlinear hydrological responses to progressive wetland degradation, ranging from 5% to 90% loss. The results reveal a strong nonlinear relationship ($R^2 = 0.997$) between wetland loss and peak discharge, with a clear acceleration beyond the 25–30% loss where system stability becomes failed. At 90% wetland loss, peak discharge increased by 109% while lag time decreased by 47%, reducing flood warning time by approximately 29 hours. This identifies a critical threshold beyond which system stability deteriorates rapidly, supporting the CAS-based hypothesis that watershed responses are not proportional to landscape change.

4.4 Hysteresis and Irreversibility in Hydrological Recovery under Wetland Restoration

The ecosystem restoration literature indicates that the structural and functional recovery of wetlands is often slow and incomplete, with systems frequently taking decades to approach reference conditions (Jones et al., 2018; Cadier et al., 2020). The concept of hysteresis has been well established both theoretically and empirically in ecological systems, particularly in lakes and other dynamic environments (Scheffer et al., 2001; Suding & Hobbs, 2009).

However, while the ecological recovery of wetlands has been extensively studied, hydrological functions, especially flood attenuation are often assumed rather than explicitly quantified in restoration assessments (Kadykalo & Findlay, 2016; Meli et al., 2014). Furthermore, many existing ecosystem service models and spatially distributed hydrological models do not incorporate hysteresis or threshold dynamics, instead relying on assumptions of linear and reversible relationships between wetland extent and flood regulation capacity (Craft et al., 2003; Maes et al., 2024). As a result, the potential irreversibility of flood attenuation services under progressive wetland loss remains insufficiently tested and understood.

The fourth objective investigated hysteresis and system memory through equivalent restoration scenarios. The findings confirms the existence of a significant hysteresis effect (HI = 0.66), indicating that only 34% of the flood attenuation function lost by wetlands can be regained through restoration efforts of the same magnitude. The Normalized Hysteresis Area Index (NHAI = 47.4%) indicates that nearly half of the cumulative hydrological impact of degradation remains irrecoverable even under equivalent restoration efforts. Path dependency analysis further demonstrated that while low-intensity degradation may be compensable, moderate to high disturbance

leads to persistent residual impacts. These findings provide quantitative evidence that watershed hydrological systems exhibit memory and do not follow reversible trajectories.

5. CONCLUSION

This study assessed watershed-scale hydrological processes using a SWAT+ modelling framework, in which natural marshes and paddy fields were represented as distinct wetland environments, while the watershed was conceptualized as a Complex Adaptive System. The results demonstrate that wetlands function as important yet limited storage components within the hydrological system. During major flood events, a substantial retention deficit was observed (210×10^5 m³), with overall retention efficiency ranging between 18% and 34%. These findings indicate that existing wetland systems are already operating under constrained storage conditions, particularly in downstream areas where excess flows and hydrological stress are more pronounced.

The analysis further reveals a strongly nonlinear relationship between wetland loss and peak discharge. While initial reductions in wetland area result in moderate increases in flood response, a critical threshold emerges at approximately 25–30% wetland loss, beyond which system stability deteriorates rapidly. Under extreme loss conditions (90%), peak discharge increases by 109%, accompanied by a 47% reduction in lag time (approximately 29 hours), significantly reducing flood response time. In addition, the results highlight the presence of hysteresis in hydrological recovery. Restoration of wetlands does not produce proportional improvements in flood attenuation, with only about 34% of the lost function recovered under equivalent restoration scenarios. This indicates that hydrological resilience is path-dependent, and that degradation leads to partially irreversible impacts on watershed behaviour.

The findings collectively demonstrate that wetlands provide a critical but insufficient flood attenuation service under increasing hydrological pressures. The observed nonlinear dynamics, threshold behaviour, and hysteresis effects emphasize that incremental wetland loss can lead to disproportionate and rapidly escalating flood risks. Consequently, maintaining existing wetland systems is substantially more effective than attempting to restore them after degradation.

REFERENCES

Acreman, M. C., & Holden, J. (2013). How wetlands affect floods. Wetlands, 33(5), 773–786. https://doi.org/10.1007/s13157-013-0473-2

Al-Attabi, Z., Xu, Y., Tso, G., & Narayan, S. (2023). The impacts of tidal wetland loss and coastal development on storm surge damages to people and property: a Hurricane Ike case-study. Scientific Reports, 13(1), 4620. https://doi.org/10.1038/s41598-023-31409-x

Armoa, O. L. B., Arnold, J. G., Bieger, K., Sauvage, S., & Sánchez-Pérez, J. M. (2024). Large wetlands representation in SWAT+: the case of the Pantanal in the Paraguay River Basin. Frontiers in Water, 6. https://doi.org/10.3389/frwa.2024.1451648

Arnold, J. G., Bieger, K., White, M. J., Srinivasan, R., Dunbar, J. A., & Allen, P. M. (2018). Use of decision tables to simulate management in SWAT+. Water, 10(6), 713. https://doi.org/10.3390/w10060713

Bouzidi, N., & Pérez-Blanco, C. D. (2025). A dynamic hydro-economic model to assess the effectiveness and economic benefits and costs of wetland restoration and creation. Ecosystem Services, 73, 101737.

Bullock, A., & Acreman, M. (2003). The role of wetlands in the hydrological cycle. Hydrology and Earth System Sciences, 7(3), 358–389. https://doi.org/10.5194/hess-7-358-2003

Cadier, C., Bayraktarov, E., Piccolo, R., & Adame, M. F. (2020). Indicators of Coastal Wetlands Restoration Success: A Systematic review. Frontiers in Marine Science, 7. https://doi.org/10.3389/fmars.2020.600220

Chen Y., Wang B., Pollino C. A., Cuddy S. M., Merrin L. E., and Huang C. (2014), Estimate of flood inundation and retention on wetlands using remote sensing and GIS, Ecohydrol., 7, 1412–1420, doi: 10.1002/eco.1467

Chow, V.T. (1964) Handbook of Applied Hydrology. McGraw-Hill Book Company, New York. - References - Scientific Research Publishing. (n.d.). https://www.scirp.org/reference/referencespapers?referenceid=1685703

Chu, N. T. W., & Shirmohammadi, N. A. (2004). Evaluation of the SWAT models hydrology component in the Piedmont physiographic region of Maryland. Transactions of the ASAE, 47(4), 1057–1073. https://doi.org/10.13031/2013.16579

Craft, C., Megonigal, P., Broome, S., Stevenson, J., Freese, R., Cornell, J., & Sacco, L. Z. a. J. (2003). The Pace of Ecosystem Development of Constructed Spartina alterniflora Marshes. Ecological Applications, 13(5), 1417–1432. https://www.jstor.org/stable/4134723

Dadson, S. J., Hall, J. W., Murgatroyd, A., Acreman, M., Bates, P., Beven, K., Heathwaite, L., Holden, J., Holman, I. P., Lane, S. N., O'Connell, E., Penning-Rowsell, E., Reynard, N., Sear, D., Thorne, C., & Wilby, R. (2017). A restatement of the natural science evidence concerning catchment-based 'natural' flood management in the UK. Proceedings of the Royal Society A: Mathematical, Physical and Engineering Sciences, 473(2199), 20160706. https://doi.org/10.1098/rspa.2016.0706

Davis, T. J., Blasco, D., & Carbonell, M. (1997). The Ramsar Convention manual : a guide to the Convention on wetlands (Ramsar, Iran, 1971). https://portals.iucn.org/library/node/7298

Dona, C. G. W., Mohan, G., Fukushi, K., & Dissanayaka, N. (2025). Exploring the economic and environmental benefits of Colombo wetlands in urban planning with nature-based solutions. Societal Impacts, 5, 100106.

e Sousa, R. D. C., & Miranda, O. L. (2018). Incorporating wetlands in hydrologic and hydraulic models for flood zone delineation: An application to Durán, Ecuador. International Journal of Disaster Risk Reduction, 28, 375-383.

England, J. F., Cohn, T. A., Faber, B. A., Stedinger, J. R., Thomas, W. O., Veilleux, A. G., Kiang, J. E., & Mason, R. R. (2018). Guidelines for determining flood flow frequency — Bulletin 17C. Techniques and Methods. https://doi.org/10.3133/tm4b5

Evenson, G. R., Golden, H. E., Lane, C. R., McLaughlin, D. L., & D'Amico, E. (2018). Depressional wetlands affect watershed hydrological, biogeochemical, and ecological functions. Ecological Applications, 28(4), 953–966. https://doi.org/10.1002/eap.1701

Gentine, P., Troy, T. J., Lintner, B. R., & Findell, K. L. (2012). Scaling in Surface Hydrology: Progress and challenges. Wiley Online Library. https://doi.org/10.1111/j.1936-704X.2012.03105.x

Golden, H. E., Lane, C. R., Amatya, D. M., Bandilla, K. W., Kiperwas, H. R., Knightes, C. D., & Ssegane, H. (2014). Hydrologic connectivity between geographically isolated wetlands and surface water systems: A review of select modeling methods. Environmental Modelling & Software, 53, 190–206. https://doi.org/10.1016/j.envsoft.2013.12.004

Guilhen, J., Parrens, M., Sauvage, S., Santini, W., Mercier, F., Bitar, A. A., Fabre, C., Martinez, J., & Sànchez-Pérez, J. (2022). Estimation of the Madeira floodplain dynamics from 2008 to 2018. Frontiers in Water, 4. https://doi.org/10.3389/frwa.2022.952810

Gupta, H., Sorooshian, S., & Yapo, P. O. (1999). Status of automatic calibration for hydrologic models: comparison with multilevel expert calibration. ResearchGate. https://doi.org/10.1061/(ASCE)1084-0699(1999)4:2(135)

Hao, L., Sun, G., Liu, Y., Wan, J., Qin, M., Qian, H., Liu, C., Zheng, J., John, R., Fan, P., & Chen, J. (2015). Urbanization dramatically altered the water balances of a paddy field-dominated basin in southern China. Hydrology and Earth System Sciences, 19(7), 3319–3331. https://doi.org/10.5194/hess-19-3319-2015

Holling, C. S. (2001). Understanding the complexity of economic, ecological, and social systems. Ecosystems, 4(5), 390–405. https://doi.org/10.1007/s10021-001-0101-5

IUCN Sri Lanka Country Office. (2004). Wetland conservation in Sri Lanka: Proceedings of the National Symposium on Wetland Conservation and Management. IUCN – The World Conservation Union.

Jansson, Å., Folke, C., & Langaas, S. (1998). Quantifying the nitrogen retention capacity of natural wetlands in the large-scale drainage basin of the Baltic Sea. Landscape ecology, 13(4), 249-262.

Jing, H., Liu, J., Zhang, Q., Wang, Z., Pang, X., & Xu, X. (2025). Adaptive wetland management: Insights from nonlinear dynamics between vegetation and hydrological variables. Ecological Indicators, 177, 113797. https://doi.org/10.1016/j.ecolind.2025.113797

Jones, H. P., Jones, P. C., Barbier, E. B., Blackburn, R. C., Benayas, J. M. R., Holl, K. D., McCrackin, M., Meli, P., Montoya, D., & Mateos, D. M. (2018). Restoration and repair of Earth's damaged ecosystems. Proceedings of the Royal Society B Biological Sciences, 285(1873), 20172577. https://doi.org/10.1098/rspb.2017.2577

Kadykalo, A. N., & Findlay, C. S. (2016). The flow regulation services of wetlands. Ecosystem Services, 20, 91–103. https://doi.org/10.1016/j.ecoser.2016.06.005

Kamruzzaman, M., Hwang, S., Choi, S. K., Cho, J., Song, I., Jeong, H., ... & Yoo, S. H. (2020). Prediction of the effects of management practices on discharge and mineral nitrogen yield from paddy fields under future climate using APEX-paddy model. Agricultural water management, 241, 106345.

Krnáčová, Z., Barančoková, M., & Labuda, M. (2025). Quantification of Soil Water Retention Capacity in the Protected Water Management Area Žitný Ostrov (Slovakia). Agriculture, 15(5), 563. https://doi.org/10.3390/agriculture15050563

Kudo, R., Masumoto, T., & Horikawa, N. (2015). Modeling of Paddy Water Management with Large Reservoirs in Northeast Thailand and its Application to Climate Change Assessment. Japan Agricultural Research Quarterly JARQ, 49(4), 363–376. https://doi.org/10.6090/jarq.49.363

Kumar, S., Agarwal, A., Villuri, V. G. K., Pasupuleti, S., Kumar, D., Kaushal, D. R., ... & Sivakumar, B. (2021). Constructed wetland management in urban catchments for mitigating floods. Stochastic Environmental Research and Risk Assessment, 35(10), 2105-2124.

Levin, S. A. (1998). Ecosystems and the biosphere as complex adaptive systems. Ecosystems, 1(5), 431–436. https://doi.org/10.1007/s100219900037

Lopes, B. S., Corrêa, K. a. B., Ogasawara, M. E. K., Precinoto, R. S., Cassiano, C. C., Sell, B. M., Melo, R. S., Oliveira, P. C. D. R., & De Barros Ferraz, S. F. (2022). How does land use cover change affect hydrological response in the Atlantic Forest? Implications for ecological restoration. Frontiers in Water, 4. https://doi.org/10.3389/frwa.2022.998349

Maes, S. L., Perring, M. P., Cohen, R., Akinnifesi, F. K., Bargués-Tobella, A., Bastin, J., Bauters, M., Bernardino, P. N., Brancalion, P. H. S., Bullock, J. M., Ellison, D., Fayolle, A., Fremout, T., Gann, G. D., Hishe, H., Holmgren, M., Ilstedt, U., Mahy, G., Messier, C., . . . Muys, B. (2024). Explore before you restore: Incorporating complex systems thinking inecosystem restoration. Besjournals. https://doi.org/10.1111/1365-2664.14614

Makungu, E., & Hughes, D. A. (2021). Understanding and modelling the effects of wetland on the hydrology and water resources of large African river basins. Journal of Hydrology, 603, 127039.

Mallawatantri, A. (2016). Medium- to long-term multi-stakeholder strategy and action plan for management and conservation of the Kelani River Basin (2016–2020): Natural resource profile of the Kelani River Basin. IUCN Sri Lanka Country Office. https://iucn.org/resources/publication/medium-long-term-multi-stakeholder-strategy-and-action-plan-management-and-0

McMillan, H. (2022). A taxonomy of hydrological processes and watershed function. Hydrological Processes, 36(3). https://doi.org/10.1002/hyp.14537

Meli, P., Benayas, J. M. R., Balvanera, P., & Ramos, M. M. (2014). Restoration enhances Wetland biodiversity and ecosystem service supply, but results are Context-Dependent: a Meta-Analysis. PLoS ONE, 9(4), e93507. https://doi.org/10.1371/journal.pone.0093507

Mereta, S. T., De Meester, L., Lemmens, P., Legesse, W., Goethals, P. L., & Boets, P. (2020). Sediment and nutrient retention capacity of natural riverine wetlands in Southwest Ethiopia. Frontiers in Environmental Science, 8, 122.

Mitsch, W. J., & Gosselink, J. G. (2015). Wetlands, 5th edition. ResearchGate. https://www.researchgate.net/publication/271643179_Wetlands_5th_edition

Moriasi, D. N., Arnold, J. G., Van Liew, M. W., Bingner, R. L., Harmel, R. D., & Veith, T. L. (2007). Model evaluation guidelines for systematic quantification of accuracy in watershed simulations. *Transactions of the ASABE, 50*(3), 885–900. https://doi.org/10.13031/2013.23153

Mukherjee, K., & Pal, S. (2020). Hydrological and landscape dynamics of floodplain wetlands of the Diara region, Eastern India. Ecological Indicators, 121, 106961. https://doi.org/10.1016/j.ecolind.2020.106961

Nash, J., & Sutcliffe, J. (1970). River flow forecasting through conceptual models part I — A discussion of principles. Journal of Hydrology, 10(3), 282–290. https://doi.org/10.1016/0022-1694(70)90255-6

Opperman, J. J., Luster, R., McKenney, B. A., Roberts, M., & Meadows, A. W. (2009). Ecologically functional floodplains: Connectivity, flow regime, and scale. Journal of the American Water Resources Association, 45(1), 211–226. https://doi.org/10.1111/j.1752-1688.2008.00299.x

Padmanabhan, G., & Bengtson, M. L. (2001). Assessing the influence of wetlands on flooding. In Wetlands Engineering & River Restoration 2001 (pp. 1-12).

Page, B., Badiou, P., & Steele, O. (2023). Nutrient retention of newly restored wetlands receiving agricultural runoff in a temperate region of North America. Ecological Engineering, 195, 107060.

Phillips, J. D. (2003). Sources of nonlinearity and complexity in geomorphic systems. Progress in Physical Geography Earth and Environment, 27(1), 1–23. https://doi.org/10.1191/0309133303pp340ra

Qian, S. S., Arend, K. K., Jacquemin, S. J., Sullivan, S. M. P., & Kowalski, K. P. (2023). Estimating phosphorus retention capacity of flow-through wetlands. Ecological Engineering, 187, 106869.

Scheffer, M., Carpenter, S., Foley, J., Folke, C., & Walker, B. (2001). Catastrophic shifts in ecosystems. https://www.semanticscholar.org/paper/Catastrophic-shifts-in-ecosystems-Scheffer Carpenter/faa8d78e3cbb1f1e814a2808c56f8d08f0a06c74

Schottler, S. P., Ulrich, J., Belmont, P., Moore, R., Lauer, J. W., Engstrom, D. R., & Almendinger, J. E. (2013). Twentieth century agricultural drainage creates more erosive rivers. Hydrological Processes, 28(4), 1951–1961. https://doi.org/10.1002/hyp.9738

Singh, J., Knapp, H. V., Arnold, J., & Demissie, M. (2005). Hydrological modeling of the Iroquois river watershed using HSPF and SWAT. JAWRA Journal of the American Water Resources Association, 41(2), 343–360. https://doi.org/10.1111/j.1752-1688.2005.tb03740.x

Sohoulande, C. D., Szogi, A. A., Novak, J. M., Stone, K. C., Martin, J. H., & Watts, D. W. (2022). Long-term nitrogen and phosphorus outflow from an instream constructed wetland under precipitation variability. Sustainability, 14(24), 16500.

Suding, K. N., & Hobbs, R. J. (2009). Threshold models in restoration and conservation: A developing framework. Trends in Ecology & Evolution, 24(5), 271–279. https://doi.org/10.1016/j.tree.2008.11.012

Surasinghe, T., Kariyawasam, R., Sudasinghe, H., & Karunarathna, S. (2019). Challenges in biodiversity conservation in a highly modified tropical river basin in Sri Lanka. Water, 12(1), 26. https://doi.org/10.3390/w12010026

Vreugdenhil, M., Széles, B., Salinas, J. L., Strauß, P., Oismueller, M., Hogan, P., Wagner, W., Parajka, J., & Blöschl, G. (2022). Non-linearity in event runoff generation in a small agricultural catchment. Hydrological Processes, 36(8), e14667. https://doi.org/10.1002/hyp.14667

Wen, L., Macdonald, R., Morrison, T., Hameed, T., Saintilan, N., & Ling, J. (2013). From hydrodynamic to hydrological modelling: Investigating long-term hydrological regimes of key wetlands in the Macquarie Marshes, a semi-arid lowland floodplain in Australia. Journal of hydrology, 500, 45-61.

Xia, Q., Liu, P., Fan, Y., Cheng, L., An, R., Xie, K., & Zhou, L. (2022). Representing irrigation processes in the Land Surface-Hydrological Model and a case study in the Yangtze River Basin, China. Journal of Advances in Modeling Earth Systems, 14(7). https://doi.org/10.1029/2021ms002653

Yi, Q., Huixin, G., Yaomin, Z., Jinlian, S., Xingyu, Z., Huize, Y., Jiaxin, W., Zhenguo, N., Liping, L., Shudong, W., Tianjie, Z., Yue, C., Zongming, W., Dehua, M., Mingming, J., Ke, G., Peng, G., Guofa, C., & Xiankai, H. (2024). Global conservation priorities for wetlands and setting post-2025 targets. Communications Earth & Environment, 5(1). https://doi.org/10.1038/s43247-023-01195-5

Zehe, E., & Sivapalan, M. (2009). Threshold behaviour in hydrological systems as (human) geo-ecosystems: manifestations, controls, implications. Hydrology and Earth System Sciences, 13(7), 1273–1297. https://doi.org/10.5194/hess-13-1273-2009

Zhang, L., & Mitsch, W. J. (2005). Modelling hydrological processes in created freshwater wetlands: an integrated system approach. Environmental Modelling & Software, 20(7), 935-946.

STATEMENTS & DECLARATIONS

Funding

The authors declare that no funds, grants, or other support were received during the preparation of this manuscript

Competing Interests

The authors have no relevant financial or non-financial interests to disclose.

Author Contributions

L.O.H. Perera made substantial contributions to the conception of the study, data analysis, validation, interpretation of results, and drafting of the original manuscript.

E.J. Warusavitharana contributed through supervision of the research and critical review and editing of the manuscript.

Data Availability

The datasets generated during and/or analysed during the current study are available from the corresponding author on reasonable request

APPENDICES

Appendix A - Wetland loss scenarios: Area changes and conversion priorities

Scenario	Wetland Area	Special Considerations
5% Loss	210 Sq.km Paddy - ~3% loss Marsh - ~2% loss	• Only immediate urban edge wetlands affected • Minimal impact on the ecosystem • Natural urban expansion pattern
10% Loss	199 Sq.km Paddy - ~6% loss Marsh - ~4% loss	• Wetlands within a 1-pixel buffer of urban converted • Small edge patches removed • Major wetland areas fully protected
15% Loss	188 Sq. km Paddy - ~9% loss Marsh - ~6% loss	• 1–2-pixel buffer from urban areas • Rice paddies near cities prioritized • Maintains all major wetland complexes
20% Loss	177 Sq.km Paddy - ~13% loss Marsh - ~7% loss	• Extends to a 2-pixel buffer around urban • Small, isolated patches (<5 pixels) converted • Noticeable agricultural wetland loss
25% Loss	165.8 Sq.km Paddy - ~16% loss Marsh - ~9% loss	• 2–3-pixel buffer conversion • Patches <7 pixels vulnerable • Minor fragmentation begins
30% Loss	154.7 Sq.km Paddy - ~20% loss Marsh - ~10% loss	• 3-pixel urban buffer affected • Small clusters (<10 pixels) converted • Rice paddies were significantly reduced • Fragmentation becomes visible
35% Loss	143.5 Sq.km Paddy - ~23% loss Marsh - ~12% loss	• 3–4-pixel buffer from urban • Isolated patches <12 pixels lost • Moderate fragmentation
40% Loss	132.5 Sq.km Paddy - ~26% loss Marsh - ~14% loss	• 4-pixel buffer conversion • Fragments of larger wetland complexes • Small patches (<15 pixels) eliminated
45% Loss	121.4 Sq.km Paddy - ~30% loss Marsh - ~15% loss	• 5-pixel buffer from urban • Medium patches (<20 pixels) removed • Major connectivity losses
50% Loss	110.4 Sq.km Paddy - ~33% loss Marsh - ~17% loss	• Half of the wetlands have been converted • Only complexes >25 pixels secure • Severe fragmentation
60% Loss	88.4 Sq.km Paddy - ~40% loss Marsh - ~20% loss	• Most accessible wetlands gone • Clusters <35 pixels converted • Only remote areas intact
70% Loss	66.2 Sq.km Paddy - ~47% loss Marsh - ~23% loss	• Only protected and remote wetlands remain • No functional connectivity • Rice paddies have been mostly eliminated
80% Loss	44.2 Sq.km Paddy - ~55% loss Marsh - ~25% loss	• Only core conservation areas remain • Complete isolation of remnants • Agricultural wetlands are nearly extinct

90% Loss	22.1 Sq.km Paddy - ~65% loss Marsh - ~25% loss	• Only the most remote/protected wetlands survive • All rice paddies in accessible areas are gone • Maximum urbanization scenario

Appendix B - Wetland Restoration Analysis: Area changes & Restoration priorities

Scenario	Wetland Area	Special Considerations
5% Restoration	55.6 Sq.km	• Only selected pixels directly adjacent to main channels (Stream Order >3) • Strictly targets non-agricultural scrub within 50m of waterways
10% Restoration	66.8 Sq.km	• Filled gaps between existing wetland patches. • Prioritized unused land contiguous with existing marsh
15% Restoration	77.9 Sq.km	• Connects fragmented patches within the same sub-basin. • Targets potential areas excluding urban lands.
20% Restoration	89.1 Sq.km	• Targets low-lying depressions that are currently unused/abandoned
25% Restoration	100.2 Sq.km	• Targets CRGR on extremely flat terrain (<1% slope) near river reaches
30% Restoration	111.3 Sq.km	• Converts scrub edges bordering urban zones to act as filtration strips
35% Restoration	122 Sq.km	• Establishes 100m buffer zones around existing wetlands
40% Restoration	132.7 Sq.km	• Creates continuous wetland corridors linking major water bodies
45% Restoration	143.4 Sq.km	• Extends restoration to areas with <3% slope
50% Restoration	154.2 Sq.km	• Reaches 50% restoration of identified potential restorable areas (PRA).
60% Restoration	177.9 Sq.km	• Establishes wetland complexes at all major channel confluences
70% Restoration	200.6 Sq.km	• Adjacent areas to paddy fields were considered
80% Restoration	222.3 Sq.km	• Nearly all eligible barren land and scrub within the <5% slope limit converted
90% Restoration	245.3 Sq.km	• Maximum feasible restoration excluding only prime agricultural land, forests, and urban cores